RSC Advances

REVIEW

View Article Online
View Journal | View Issue

Cite this: *RSC Adv.*, 2019, **9**, 40642

Application of graphene derivatives and their nanocomposites in tribology and lubrication: a review

Jianlin Sun and Shaonan Du *

Reducing friction and increasing lubrication are the goals that every tribologist pursues. Accordingly, layered graphene materials have attracted great research interest in tribology due to their anti-friction, anti-wear and excellent self-lubricating properties. However, recent studies have found that other forms of graphene derivatives not only perform better in tribological and lubricating applications, but also solve the problem of graphene being prone to agglomeration. Based on a large number of reports, herein, we review the research progress on graphene derivatives and their nanocomposites in tribology and lubrication. In the introduction, the topic of the article is introduced by highlighting the hazards and economic losses caused by frictional wear and the excellent performance of graphene materials in the field of lubrication. Then, by studying the classification of graphene materials, the research status of their applications in tribology and lubrication is introduced. The second chapter introduces the application of graphene derivatives in improving tribological properties. The main types of graphene are graphene oxide (GO), doped graphene (doped elements such as nitrogen, boron, phosphorus, and fluorine), graphene-based films, and graphene-based fibers. The third chapter summarizes the application of graphene-based nanocomposites in improving friction and anti-wear and lubrication properties. According to the different functional modifiers, they can be divided into three categories: graphene–inorganic nanocomposites (sulfides, metal oxides, nitrides, metal nanoparticles, and carbon-containing inorganic nanoparticles), graphene–organic nanocomposites (alkylation, amine functionalization, ionic liquids, and surface modifiers), and graphene–polymer nanocomposites (carbon chain polymers and heterochain polymers). Graphene not only exhibits an excellent performance in traditional processing and lubrication applications, but the fourth chapter proves that it has a good application prospect in the

Received 23rd July 2019
Accepted 21st November 2019

DOI: 10.1039/c9ra05679c

rsc.li/rsc-advances

School of Materials Science and Engineering, University of Science and Technology Beijing, Beijing 100083, PR China. E-mail: dsnbeikeda@126.com

Professor Jianlin Sun (born in China in 1963) obtained Bachelor's degree from the National Defense University of Technology in 1985 and continued his studies for Master's and PhD degrees in the Central South University of Technology, Changsha, China. Currently, he is a Professor and researcher in the University of the University of Science and Technology, Beijing, China. He is very good at nano-friction and lubrication, evaluating the lubrication mechanism of different nanomaterials, surface quality control and nano-lubrication performance during metal rolling. In the direction of friction and lubrication, he has written 3 books and published 138 articles and 25 patents.

Mr Shaonan Du (born in China in 1993) will obtain his Master's degree from the University of Science and Technology Beijing, China, in 2019, and is interested in continuing his Ph.D. He is very good at the preparation of graphene-based nanocomposites. He has studied the dispersion stability, friction and lubrication properties of graphene-based nanocomposites. He has published two articles as the first author and correspondent so far.

field of ultra-low friction and superlubricity. In the application part of the fifth chapter, the lubrication mechanism proposed by graphene as a nano-lubricant is introduced first; then, the main application research status is summarized, including micro-tribology applications, bio-tribology applications, and liquid lubrication additive applications. The last part is based on the following contents. Firstly, the advantages of graphene-based nanocomposites as lubricants and their current shortcomings are summarized. The challenges and prospects of the commercial applications of graphene-based nanocomposites in tribology and lubrication are further described.

1 Introduction

Research in the field of friction and lubrication has received increasing attention; however, it still faces considerable challenges. For example, the energy loss caused by friction accounts for 1/3 of the world's industrial energy consumption and 80% part failure is caused by wear and tear.[1,2] Friction and wear not only affect the operation and maintenance of traditional industrial equipment, machines, part quality and life, but also affect micro-devices and biological and human applications.[3,4] Currently, the understanding of the microscopic mechanism of friction, wear and lubrication and the development of new lubricating materials have made great progress, significantly reducing friction and wear and improving lubrication protection. The way to control friction and wear at different scales is different. Tribological optimization and improvement of materials at the micro–nano level is more effective.[5] Lubrication in machinery and industrial applications is an effective measure to control friction and wear.[6] Also, with the development and application of new lubricant additives, the ability of lubricants to reduce friction and wear can be further improved.

Graphene, a two-dimensional (2D) carbon crystal with the honeycomb lattice structure, has attracted great research interest in many different fields due to its outstanding performance.[7–10] Inside the graphene sheet, the C–C bond is sp^2 hybridized, and the bond energy is high. The graphene layers are connected by a weak interaction force, van der Waals force.[11] Considering its high Young's modulus and excellent self-lubricating properties, graphene is considered to be an excellent candidate for reducing friction, wear and improving lubrication.[12,13] However, there are some problems with graphene lubrication applications under certain conditions. When graphene is used in water-based and oil-based lubrication systems, it tends to agglomerate and precipitate.[14,15] In addition, graphene raw materials are difficult to be uniformly distributed as modifiers in various alloys and polymer matrices to improve performance.[16] Graphene oxide (GO), the special derivative of graphene, contains abundant oxygen-based groups. It is evenly dispersed to enhance lubrication, while also being functionalized by specific chemical molecular groups to improve its suitability. Currently, numerous graphene derivatives and their nanocomposites have been studied and prepared as new anti-wear and friction reducing agents and lubricant additives (Table 1). The surface modification technique brings two advantages to the graphene material: first, it can be uniformly dispersed in the base liquid medium; and second, its unique properties can be applied to special environments. In addition, the surface functionalization of graphene indirectly increases the distance between graphene sheets, allowing them to exist in a single layer in a matrix. This has a certain significance for studying the interaction between the surface of graphene nanosheets and other materials.

Graphene derivatives and their nanocomposites can be roughly divided into four categories: graphene derivatives, graphene–inorganic nanocomposites, graphene–organic nanocomposites, and graphene–polymer nanocomposites. They have been extensively researched both theoretically and experimentally and shown to retain the graphene matrix structure.[26] Thus, these materials also have excellent mechanical and chemical properties.[27–29]

This review focuses on the use of the above four graphene-based nanomaterials in tribology and lubrication to emphasize their respective mechanisms of friction reduction, wear resistance and lubrication. First, we summarize the application examples of graphene derivatives and their nanocomposites. Subsequently, the latest research on graphene-based materials in ultra-low friction and superlubricity are evaluated. Next, the application of graphene derivatives and their nanocomposites in the micro-tribology, bio-tribology and industrial friction lubrication industries will be discussed in detail. Finally, the significant challenges and possible solutions for applying these materials are presented.

2 Graphene derivatives for improving tribological properties

The excellent mechanical and chemical properties of graphene have aroused widespread interest among researchers in the field of tribology. The ideal quasi-two-dimensional structure and excellent properties of graphene and the chemical reactivity of its six-membered carbon ring structures cause graphene to have a large number of derivative applications. Novel graphene derivatives are prepared by changing the spatial configuration, regulating the electronic structure, and performing functional processing. At present, researchers have achieved specific surface functionalization of graphene by modifying functional groups on the surface of graphene. By changing the spatial conformation of graphene, macroscopic one-, two-, and three-dimensional graphene substrates can be obtained, such as graphene films, and graphene fibers. The regulation of the structure and properties of graphene can also be achieved by techniques such as element doping and hydrogenation.

2.1 Graphene oxide

Industrially, graphite is usually selected to prepare GO. Therefore, the choice of GO for research has inherent cost advantages

Table 1 Graphene derivatives and their nanocomposites serve as friction reducing agents and lubricant additives

Graphene nanocomposite	Experimental method	Tribological properties		Group	Application	Ref.
		Friction coefficient (μ)	Wear			
MoS_2/GO	Using an MS-T3000 ball-on-disk apparatus	Pure oil $\mu = 0.0915$, 1.0 wt% MoS_2 $\mu = 0.0685$, 1.0 wt% MoS_2/GO $\mu = 0.0557$	Wear track width (μm) MoS_2 202.33 187.57 219.33 MoS_2/GO 190.28 (0.5 wt%) 132.32 (1.0 wt%) 182.83 (2.0 wt%)	Song *et al.*	As additive in sunshine oil	17
TiAl matrix/graphene	Using an HT-1000 ball-on-disk high temperature tribometer	Reduction in COF: WS_2 32.07%, 28.57%, MoO_3 35.85%, 30.36%, MLG 39.62%, 35.71%	Reduction in the wear rates: WS_2 3.22%, 6.07%, MoO_3 5.56%, 10.44%, MLG 89.16%, 81.79%	Xu *et al.*	As solid lubricants with excellent self-lubricating	18
Carbon nitride/graphene	Using a home-built ball-on-disk apparatus	In N_2 gas stream the COF reached stable value of 0.05, which was one-third of the value in ambient air	The wear scars of the surfaces were covered by large amount of tribofilms after sliding in N_2 gas stream	Wang *et al.*	Used as a low friction nanocomposite coating	19
Cu/reduced graphene oxide	Using a four-ball wear tester	Pure PAO $\mu = 0.10$, 1.0 wt% Cu/rGO PAO $\mu = 0.055$	Wear scare diameters (WSD): 0.5 wt% Cu/rGO added the WSD reduced from 0.75 mm to 0.35 mm	Jia *et al.*	As additive in poly-alpha-olefin (PAO)	20
Boron carbide/graphene	Using the ball-on-flat technique	0.47–0.60 at a load of 5 N, 0.34–0.54 at a load of 30 N, 0.35–0.58 at a load of 50 N	B_4C with the lowest content of GPLs had the highest specific wear rate at all loads	Sedlák *et al.*	As a new wear-resistant material	21
Alkylated graphene	Using a four-ball machine	With the presence of ODA-Gr, the COF was reduced by 20–26%	The wear scar diameter is reduced and is minimum at 0.06 mg mL^{-1}	Shivani *et al.*	Disperse in organic solvent	22
GO-hybrid polyurethane	Using a pin-on-disk friction wear testing machine	The average friction coefficient is decreased about 30.2% from 0.997 of neat PU/EP IPN to 0.696 of GO-hybrid PU/EP IPNs	The wear rate is decreased about two orders of magnitude. From 8.9×10^{-4} mm^3 Nm^{-1} to 4.6×10^{-6} mm^3 Nm^{-1}	Xia *et al.*	Add it to epoxy resin to reduce friction coefficient	23
Ni_3Al matrix/multilayer graphene	Using a HT-1000 pin-on-disk high temperature tribometer	The COF reduced from 0.4–0.21 with the increase of sliding speed. It is more than 30% lower than those of no graphene (0.7–0.5)	With the reinforced NMCs, wear rates reduced 70% than those NA. 0.9–1.5 $\times 10^{-5}$ mm^3 Nm^{-1} to 4.2–5.0 $\times 10^{-5}$ mm^3 Nm^{-1}	Zhai *et al.*	Improve the tribological properties of traditional engineering materials	24
Polyimide/GO	Using an MRH-03 type ring-on-block test	3 wt% GO, the COF change is 26.3%	The wear rate change of PI/GO composite with 3 wt% GO is 21.3%	Liu *et al.*	As a friction pair protective film under dry friction	25

and manufacturing process advantages. GO, which is oxygen-functionalized and solution processable graphene, has become an important additive and performance enhancing material in composite materials, and it has been widely used in tribology. It also plays an important role in water-based and oil-based nano-lubrication.

Among the nano-lubricating additive materials, graphene derivatives are currently receiving the most attention due to their unique structural advantages, physical properties and chemical properties.[30] GO as a lubricant additive is one of the most important application directions. Kinoshita *et al.* prepared GO flakes by dropping 0.01 wt% of GO dispersion onto a freshly cut mica substrate and then drying in air.[31] A single layer of GO flakes was dissolved in purified water at a concentration of 1 wt% for tribological experiments. The addition of GO particles in water improved the lubricity and provided a very low coefficient of friction of about 0.05 and no significant surface wear after 60 000 friction test cycles. Peng demonstrated by atomic force microscopy that the antifriction and antiwear properties of graphene materials are closely related to their graphite structure and surface properties.[32]

2.2 Doped graphene/graphene oxide

The doping of graphene refers to the introduction of heteroatoms into the graphite rare crystal lattice by a certain method. Theoretical and experimental results show that the selection of heteroatoms (such as N, B, P, and F) with similar atomic size can change the band structure of graphene, resulting in a metal-to-semiconductor transition. The introduction of graphene into surface defects and structural disorder increases the adsorption properties of graphene. Thus doped graphene has great application value in the research of tribology and nano-lubrication.

At present, there are many nitrogen-doped graphene thinners, and their preparation methods include plasma nitriding, chemical vapor deposition, and arc discharge. Fig. 1 shows electrical heating of graphene in an ammonia atmosphere to obtain nitrogen-doped graphene.[33] Graphene is heated to several hundred degrees celsius, and its defect sites and active edges react with ammonia to form bonds. This method barely introduces impurity into the plane, and only the edge portion hybridizes to ensure excellent in-plane conductivity. Niu *et al.* prepared boron-doped graphene (BG) *via* the pyrolysis of GO with boric acid (H_3BO_3) in an argon atmosphere at 900 °C.[34] Under this reaction condition, H_3BO_3 decomposed to produce boron oxide (B_2O_3). The boron oxide vapor can enter the graphene sheet layer, and the boron atoms replace the carbon atoms in the graphene by the reaction, thereby achieving the doping of boron atoms into the graphene lattice. As the reaction time increased, the boron content in the BG increased. After 3 h, it reached the highest value of 4.7%. For graphene, which is used as an ultra-thin lubricating protective film for machine components, it must maintain low friction and high durability. Single-layer or multilayer graphene is treated by fluorine plasma to prepare fluorinated graphene. Studies have shown that fluorinated graphene can reduce the adhesion of the friction interface and improve the durability of graphene.[35]

2.3 Graphene-based film

Self-supporting film-like materials can be used as a protective layer, adhesive layer, chemical adsorption and energy storage material, *etc.*, and have been favored in the industrial field. The microscopic two-dimensional structure of graphene makes it easy to prepare graphene-film materials with a macroscopic two-dimensional structure. By enhancing the interaction between the layers and restoring the compactness of the graphene material, high-strength, high-toughness macroscopic two-dimensional graphene materials can be obtained, which are applied in the field of thin films.

To study the properties of graphene films as solid lubricants, Wu *et al.* prepared self-assembled graphene films (SGF) based on the Marangoni effect using electrochemically stripped graphene sheets (Fig. 2).[36] A new lubrication system was developed in which graphene and graphene were in contact with each other to achieve low friction in macroscopic contact. The friction coefficient changes in three cases were investigated, namely Si_3N_4 against Si, Si_3N_4 against graphene–Si and graphene–Si_3N_4 against graphene–Si. The friction coefficient was the lowest when both friction pairs were coated with a graphene

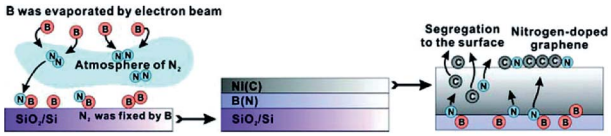

Fig. 1 Schematic diagram of the preparation of N-doped graphene. Reproduced from ref. 33 with permission from ACS, Copyright 2012.

film. Graphene films have good transferability and high-performance friction reduction behavior as lubrication systems, and thus have good prospects in engineering applications.

Since their production cost is lower than that of graphene and they also have excellent self-lubricity, GO films can also be used as solid lubricants. In particular, the functional groups contained on the surface and edges of GO enable the control of its tribological properties through surface modification. On the other hand, the degree of reduction of GO can be controlled to adjust the C/O ratio in GO to achieve different mechanical properties. These advantages have driven the preparation of GO films and their research as solid lubricants. Ou *et al.* covalently assembled rGO on the surface of a silicon crystal *via* a multi-step chemical reaction method. The micro-tribological properties of rGO were evaluated by atomic force microscopy and it was found that the rGO-coated silicon has good friction reduction and wear resistance.[37] Wei *et al.* studied the friction properties of reduced GO at different reaction temperatures, and found that the frictional difference of the prepared rGO decreased with an increase in the reduction temperature.[38]

2.4 Graphene-based fibers

As a typical two-dimensional material, it is easy to assemble graphene into two-dimensional and three-dimensional structures. If such a two-dimensional nano-thick graphene sheet can be assembled into a macroscopic one-dimensional material, a continuous graphene fiber can be prepared. It is expected to achieve a combination of macroscopic one-dimensional structure and microscopic two-dimensional structure, greatly

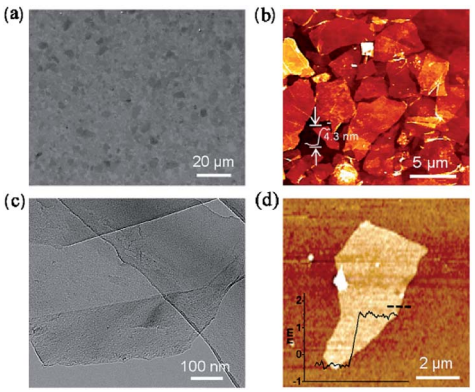

Fig. 2 (a) SEM image of SGF, (b) AFM image of SGF, (c) TEM image of graphene flakes and (d) AFM image of graphene. Reproduced from ref. 36 with permission from ACS, Copyright 2017.

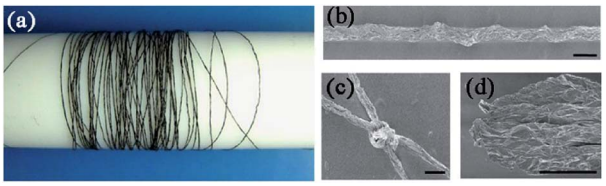

Fig. 3 (a) Four meter-long GO fibre, (b) SEM image of the fibre, (c) typical tighten knots and (d) fracture morphology of GO fibre after tensile tests. Reproduced from ref. 42 with permission from Nature, Copyright 2011.

expanding the application range of graphene. Also, because graphene has excellent mechanical and electrical properties, assembling the structure of one-dimensional macroscopic fibers based on graphene can promote its application in actual production.

Graphene-based fibers have some excellent properties such as flexibility,[39] fatigue life[40] and wear resistance.[41] The preparation of graphene fibers is typically carried out *via* a spinning process, including melt spinning, electrospinning and wet spinning. Gao's research team started from the liquid crystal structure of GO, and successfully prepared several meters of regular and regular graphene fibers and their assemblies by wet spinning, as shown in the Fig. 3.[42] GO liquid crystal is a semi-solid semi-liquid dispersion, which can be well-applied to the spinning of fibers. The ordered arrangement of graphene within the structure imparts excellent mechanical properties to the fibers and their assemblies, which further expands its application in macroscopically ordered materials.

3 Graphene-based nanocomposites for enhancing anti-wear, friction reduction and lubrication properties

Graphene is not only poorly soluble in water, but also has low solubility in most solvents. However, the main part of graphene in practical tribology and lubrication applications is its dissolution in various lubricants. Thus, to increase the solubility of graphene, a commonly used method is to introduce different modifying materials into the carbon main chain by surface modification. Surface modification is divided into covalent functionalization and non-covalent functionalization depending on how the functionalized material is attached to graphene.[43–47] In this section, functional modification materials are classified into three categories based on current research results, including inorganic, organic, and polymers. The preparation schemes and modification methods for graphene nanocomposites modified by different functional materials are introduced in detail. The effect of functionally modified materials on the tribological properties and lubricity of graphene is illustrated.

3.1 Graphene–inorganic nanocomposites

At present, the introduction of nanomaterials in the field of tribology and lubrication has been extensively studied. Graphene and GO can be modified by inorganic chemicals to form various multifunctional nanocomposites. This type of graphene-based nanocomposite exhibits unique advantages in the field of lubricant additives. Accordingly, the inorganic nanomaterials that have been studied include sulfides, metal oxides, nitrides, nano-metal particles and carbon-containing inorganic nanoparticles.

3.1.1 Sulfide-functionalized graphene. In recent years, transition metal sulfides represented by the MS_2 class have been widely used in the field of lubrication due to their special structures and excellent physical and chemical properties.[48] MS_2 has a typical three-layer structure, that is, its upper and lower layers are densely packed hexagonal sulfur atoms with a metal M layer interposed between them, and the triangular atoms of the sulfur atoms surround the M atoms. In the crystal structure, the M–S atoms are covalent bonds, and the adjacent S–M–S layers are connected by weak van der Waals forces. This special structure of the MS_2 type sulfide makes the S–M–S covalent bond in the layer have a strong binding force, and the S–S bond bonding force between the layers is weak, and it is easy to slip when subjected to external pressure. Table 2 lists the types, preparation methods and applications of sulfide–graphene nanocomposites.

An MoS_2/reduced GO hybrid material (MoS_2/rGO) was synthesized through a facile and effective hydrothermal method.[49] MoS_2 nanospheres were well attached to the creased rGO sheets. Tribological experiments showed that when the content of the composite material was 3 wt%, the lowest tribological coefficient and the most stable wear rate value were exhibited. Under high temperature conditions (600 °C), the synergistic lubrication effect of the composite material was more significant. The same method can also be used to prepare FeS_2(pyrite)/reduced GO (FeS_2/rGO) heterojunction. FeS_2 particles are well distributed on rGO nanosheets with controlled size and morphology. Also, FeS_2/rGO composites as lubricating oil additives can improve the load-carrying capacity dramatically, as well as the friction reduction and anti-wear properties of paraffin oil. This can be attributed to the unique layered structure (shown in Fig. 4) of FeS_2 and rGO.[54] The ZnS nanoparticles can be uniformly dispersed on rGO nanosheets having a diameter of several tens of nanometers by a simple and effective hydrothermal method. The ability to alter the tribological properties of epoxy coatings was due to the excellent synergistic effect between the ZnS nanoparticles and the rGO nanosheets and between the transfer films formed on the steel spheres.[57]

3.1.2 Metal oxide functionalized graphene. Nanoparticles of metal oxides in different shapes such as granules, spheres, rods and flakes, show specific functions in the field of friction reduction and anti-wear. Also, because of their low-cost synthesis, easy use, and excellent performance, metal oxide nanoparticles have attracted great research interest. For example, Song *et al.* synthesized composites of GO nanosheets and α-Fe_2O_3 nanorods through a facile hydrolysis route.[58] It was observed that the α-Fe_2O_3 nanorods had a diameter of 3–5 nm and a length of 15–30 nm in the composite. Tribological experiments showed that the base oil with α-Fe_2O_3 nanorod/GO

Table 2 Relevant information dealing with the preparation and the application of sulfide–graphene nanocomposites

Materials	Method	Tribological properties: Friction coefficient (μ)	Tribological properties: Wear	Application	Ref.
MoS_2/rGO	A facile and effective hydrothermal method	3 wt% MoS_2/rGO $\mu = 0.21$. At 600 °C, the μ was less than 0.30	Wear rate: 3 wt% MoS_2/rGO 1.07–1.90 $\times$ 10^{-5} mm^3 Nm^{-1}. At 600 °C, the wear rate was 1.07 $\times$ 10^{-5} mm^3 Nm^{-1}	Add in Fe–Ni matrix composites	49
WS_2/rGO	A simple precipitation polymerization approach	The virgin BMI $\mu = 0.42$, 0.6 wt% WS_2/rGO (min) $\mu = 0.13$, >0.6 wt% the COF shows an upward trend	Wear rate: pure BMI 16.5 $\times$ 10^{-6} mm^3 Nm^{-1}, 0.6 wt% WS_2/rGO 1.22 $\times$ 10^{-6} mm^3 Nm^{-1} reduced by 92.6%	Enhanced mechanical and tribological properties of bismaleimide resin	50
CuS/graphene	A simple one-pot hydrothermal route	CuS/graphene possesses the most outstanding peroxidase-like activity better than pure CuS		Enhanced peroxidase-like catalytic activity	51
CdS/rGO	Microwave-assisted reduction	CdS/rGO exhibit enhanced photocatalytic performance for the reduction of Cr(VI) with a maximum removal rate of 92% under visible light irradiation as compared with pure CdS (79%)		Photocatalytic reduction of Cr(VI)	52
MnS_2/rGO	A facile one-step hydrothermal route	The presence of rGO significantly enhances light absorption in the visible region between 400 and 800 nm for MnS_2/rGO hybrids		Photocatalytic	53
FeS_2/rGO	A facile and effective hydrothermal method	FeS_2, rGO, FeS_2/rGO can decrease the COF, and the tribological properties increased with the increase of GO in FeS_2/rGO	The depth and width of wear scar of 7 wt% FeS_2 are 3.5 μm and 360 μm. 7 wt% FeS_2/rGO–C are about 1.3 μm and 310 μm	Used as lubricating oil additive	54
CoS_2/graphene	A facile one-step hydrothermal route	Charge and discharge capacities of CoS_2/G are 770 and 1150 mA h g^{-1}, CoS_2 are 570 and 1000 mA h g^{-1}	40 cycles 600 mA h g^{-1} of CoS_2/G, 40 cycles below 50 mA h g^{-1} of bare CoS_2	For electrochemical lithium storage performance	55
NiS_2/graphene	A facile and economical strategy	The overpotential and charge transfer resistance of the hybrid are much lower than those of the bare NGF, MoS_2/NGF, NiS_2/NGF		For efficient overall water splitting	56

composite exhibited better tribological properties and lubricity than the base oil with GO nanosheets. By taking advantage of the design and construction of strong graphene matrix interfaces, Liu *et al.* prepared ternary nanoparticles (GNS–Fe_3O_4@-PZM) consisting of graphene, Fe_3O_4 nanoparticles and highly cross-linked polyphosphazene *via* a two-stage process consisting of co-precipitation and precipitation polymerization.[59] Subsequently, bismaleimide (BMI) matrix composites with aligned GNSFe_3O_4@PZM were fabricated under a magnetic field to take full advantage of the tribological properties of graphene. Gonzalez *et al.* depicted the wear behavior of graphene/alumina composites.[60] In their study, GO/Al_2O_3 nano-powder was prepared *via* a colloidal method. Since the presence of graphene flakes adheres to the friction surface, a self-lubricating layer was formed to provide sufficient lubrication to reduce the wear rate and friction coefficient.

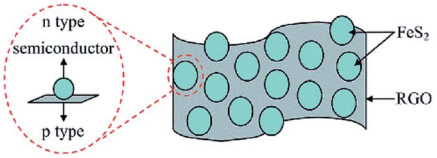

Fig. 4 Schematic diagram of FeS_2/rGO heterojunction. Reproduced from ref. 54 with permission from RSC, Copyright 2015.

Our group demonstrated the self-assembly of a GO–TiO_2 nanocomposite *via* an improved and facile solvothermal method.[61] The SEM and TEM images indicated that the TiO_2 formed was grafted on the surface of GO rather than in the form of a mixture. Also, the dispersion stability of the composite in aqueous solution was greatly improved. Subsequent experiments of tribological and rolling lubrication showed that the nanofluids with GO–TiO_2 composites had the best tribological and lubricating properties.

3.1.3 Nitride-functionalized graphene. Among engineering ceramic materials, nitrides have low density and excellent mechanical properties. Experience has shown that nitride materials perform significantly in terms of wear resistance. However, in complex tribochemical environments, these materials become very active and cause them to lose their superior performance. Considering the current trend of combining engineering ceramic materials in tribological applications and

the excellent mechanical properties and thermal stability properties of graphene materials, research on the tribological properties of nitride-functionalized graphene is also valuable.

Hvizdos *et al.* observed the wear behavior of Si_3N_4–graphene nanocomposites at room temperature by means of the ball-on-disk technique with a silicon nitride ball used as the tribological counterpart.[62] The wear rate of 3 wt% Si_3N_4–graphene was reduced by 60% compared to silicon nitride, which may be due to the fact that the graphene sheets can be strongly integrated into the matrix, making densification more difficult and increasing the nanocomposite porosity. Graphene and BN nanosheets are excellent lubricants because their flake morphology allows for infiltration and stable deposition into the friction area, preventing direct contact between the sliding surfaces. The hexagonal boron nitride functionalized using a water bath was added to the water, and even a small amount can improve the wear resistance and reduce the friction coefficient. Also, the dispersion was very stable.[63] In his Master's degree thesis, Liu demonstrated a new nanocomposite preparation technology, high energy ball milling.[64] The anti-wear performances of graphene/BN composite nanosheets were investigated. The results showed that the composite nanosheets had better wear resistance than single nanosheets.

3.1.4 Metal nanoparticle-functionalized graphene. Metal nanoparticles are often used in automotive, precision manufacturing and aerospace applications due to their special mechanical and self-lubricating properties. Functionalizing metal nanoparticles to modify the graphene can effectively utilize the advantages of the two materials in terms of lubrication. The combination of the two not only maximizes the usability of the metal nanoscale surface area, but also promotes complete dispersion of the graphene sheets. However, it has been found that due to the difference in surface energy between carbon and metal, the metal does not easily wet the graphene sheets and separate them. Therefore, preparing a metal nanoparticle–graphene material that can exist stably and uniformly disperse is a prerequisite for studying its tribological properties. Table 3 lists the metal nanoparticle–graphene nanocomposites that have been studied so far.

Au nanoparticles have a face-centered cubic crystal structure. Au nanoparticles can be successfully decorated onto the GO plate by the supercritical carbon dioxide ($ScCO_2$) fluid to synthesize Sc–Au/GO nanocomposites. Research has shown that Sc–Au/GO, as a lubricant additive in PAO6 oil, can improve tribological performance and show optimum lubricity.[66] Nano copper can be used to reduce GO. Nano-copper/rGO (Cu/rGO) composites with a small size, uniform distribution and high metal loading level can be synthesized *via* a simple one-step reduction. It was used as a lubricating oil additive to improve wear resistance by forming a friction film containing C, O, Cu and Fe on the surface of the friction pair.[65] Cheng *et al.* prepared a carboxylated GO complex with lanthanum on a silicon substrate.[70] GO nanosheets were successfully grafted onto a silicon substrate, and the lanthanum was attached to the GO plate *via* a coordination reaction. The obtained GO–La film had a low coefficient of friction and good wear resistance. Its remarkable tribological properties were attributed to the strong bonding of the film to the substrate and the special properties of the rare earth and GO sheets.

Metal nanoparticles can be decorated not only on graphene and GO nanosheets, but also on already functionalized graphene nanosheets. Cu nanoparticles with a diameter of 10–15 nm were uniformly and *in situ* modified on polydopamine (PDA)-functionalized GO nanosheets using a simple wet chemical reduction method. The nanocomposite not only had good dispersibility in the base oil, but also exhibited the lowest friction coefficient and high wear resistance when added to soybean oil at a content of 0.1 wt%. The inclusion of Cu/PDA/GO nanocomposites and their self-lubricating low shear strength friction film properties were key factors in reducing friction and preventing wear and deformation.[72]

To date, most works about metal nanoparticle–graphene nanocomposite-based lubricant additives have been concerned with noble metals. The synergistic lubrication properties of metal nanoparticle–graphene is attributed to its large surface area, unique structure, low graphene sheet force, and improved dispersion and surface adsorption properties. Metal nanoparticle/graphene nanocomposites can be used not only as excellent lubricant additive materials, but also as solid lubricants or as film lubrication due to their excellent self-lubricating properties.

3.1.5 Carbon-containing inorganic nanoparticle-functionalized graphene. Carbon nanomaterials play an important role in tribology and lubrication, and the combination of various carbon nanomaterials seems very attractive. Among the carbon nanomaterials, carbon nanotubes (CNTs)

Table 3 Relevant information dealing with the preparation and the application of metal nanoparticle–graphene nanocomposites

Material	Method	Application	Ref.
Cu/rGO	Facile one step *in situ* reduction method	As additives in poly-alpha-olefin (PAO)	65
Au/GO	Supercritical carbon dioxide ($ScCO_2$) fluid	As lubricating additive in PAO6 oil	66
Ag/graphene	Spark plasma sintering (SPS) process	As solid lubricant	67
Ni/GO	Chemical deposition with the assistance of supercritical carbon dioxide ($scCO_2$)	As lubricating additive	68
Al/graphene	Powder metallurgy method	As solid lubricant	69
La/GO	Epitaxial growth from silicon carbide	For the preparation of anti-friction and antiwear films	70
TiAl/graphene	Spark plasma sintering (SPS)	As solid lubricant	71

have attracted wide attention. The combination of one-dimensional carbon nanotubes and two-dimensional graphene materials and their applications in tribology are the most studied. For example, Shen *et al.* studied the effects of hybrids of multi-walled carbon nanotubes (MWCNTs) and GO nanosheets on the tribological properties of epoxy composites.[73] The content of MWCNTs was fixed at 0.5 phr and the GO content was between 0.05 and 0.5 phr. Several tribological experiments showed that when the GO content was 0.1 phr, the wear rate of the epoxy resin containing the nano-hybrid material was reduced by 40% compared with the pure epoxy resin.

Fullerene (C60) is a graphene-based material, representing a third allomorphic modification of carbon. It is a closed hollow cage, specifically, a pentagon consisting of 60 sp^2 hybrids of closely packed carbon atoms without any edges. The C60 fusion structure exhibits compression resistance, stability and high electron affinity and can be used in countless applications. Zhao *et al.* investigated the effects of two different shapes of functionalized C60 (FC60) and functionalized graphene (FG) on the tribological and corrosion resistance of epoxy coatings in polymer matrices.[74] Compared to pure epoxy resin, the composite coatings had a lower coefficient of friction, a wear mark area and a higher corrosion resistance. Simultaneously, due to the different shapes of the fullerenes and graphene nanomaterials, the corrosion resistance was different, and the tribological and anti-corrosion mechanisms were also different.

Carbon dots are new "zero-dimensional" carbon nanomaterials. Similarly to C60, carbon dots can also effectively prevent the aggregation of graphene. Cai *et al.* prepared carbon hybrid containing carbon quantum dots (CQD) and GO *via* the one-pot pyrolysis of citric acid (TDCA).[75] The GO was reduced to rGO by carbon dots, and a carbon dot–rGO composite was obtained, which can provide abundant carboxyl groups on the surface without affecting the dispersion stability of the material. The excellent tribological properties were due to the synergistic effect of the spherical CQDs and GO adsorbed on the sliding surface, and the high load caused more TDCA to deposit on the interface, and carbon tended to degrade and produce a more ordered structure.

In addition to forming nanocomposites with carbon elemental materials, graphene utilizes synergistic effects to create new lubrication mechanisms through the decoration of graphene with other carbon-containing nanomaterials, and these functional composites have further applications in the field of lubrication and wear resistance. Ammonium molybdate is adsorbed on the surface of GO, and Mo_2C/graphene nanocomposites can be synthesized by *in situ* carburization. It can enhance the self-lubricating performance of composite PTFE/Nomex fabrics to show the best tribological properties. The synergistic lubrication of Mo_2C nanoparticles and graphene nanosheets during sliding is the main reason for the enhancement of the tribological properties of Mo_2C/graphene nanocomposites.[76] Javier *et al.* studied the role of graphene in the friction and wear behavior of graphene/silicon carbide (SiC) composites.[77] The composite exhibited enhanced wear resistance compared to monolithic SiC, with a maximum improvement of about 70% for materials containing up to 20% by volume of graphene. The tribological behavior of GNP/SiC materials with adhesion lubrication and protective friction is related to the formation of a film.

3.2 Graphene–organic nanocomposites

The organic functionalization of graphene can be achieved by covalent and non-covalent methods. Many new studies are based on this to develop new organic materials and graphene to prepare more graphene nanocomposites with special properties. In this section, the preparation and tribological properties of alkylated graphene, amine-functionalized graphene, ionic liquid-functionalized graphene and surfactant-functionalized graphene are described.

3.2.1 Alkylated graphene. The weak van der Waals interaction between graphene sheets facilitates shearing and produces excellent lubricity. To utilize this lubricity phenomenon for lubricant development, graphene needs to be effectively dispersed in a hydrocarbon solvent, which is the main component of lubricating oil. By forming an amide bond on the edge of the GO, GO is covalently functionalized with an alkylamine anchored to the graphene nanosheet. For example, the covalent interaction of octadecyltrichlorosilane (OTCS) and octadecyltriethoxysilane (OTES) produced alkylated GO/rGO. The van der Waals interaction between the octadecyl chain of the alkylated GO/rGO and the octadecyl chain of the polyol ester allowed the alkylated GO/rGO to be dispersed in the polyol base oil. Analysis of the worn surface revealed that the shear-induced deposition of graphene-based friction films reduced the friction and protected the friction interface from wear.[78] Fig. 5 shows the covalent bond grafting of 1-dodecyl mercaptan and *tert*-dodecyl mercaptan with the carboxyl group of GO to prepare two lubricant additives (GO-D and GO-T).[79] The GO-D and GO-T sheets were stably dispersed in rapeseed oil. GO-D and GO-T sheets can be presented on the friction surface of the steel ball to form an adsorption film, exhibiting excellent anti-friction and anti-wear properties as well as extreme pressure properties.

In addition to being used as a lubricant additive, alkylated graphene can also be used for lubrication and protection purposes by self-assembling synthetic films on graphene or GO sheets. The OTS was grafted onto the GO-based bilayer

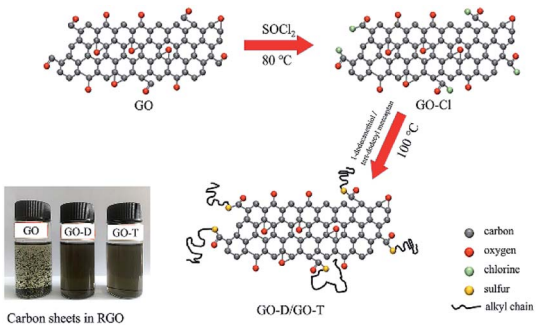

Fig. 5 Schematic of the synthesis of GO-D and GO-T. Reproduced from ref. 79 with permission from Elsevier, Copyright 2018.

membrane by condensation between the Si–OH and C–OH hydroxylated octadecyltrichlorosilane (OTS) on the GO surface. Microscopic and macroscopic tribological experiments were performed using AFM and a UMT friction tester. The results showed that the film had low adhesion and greatly reduced the friction at the microscopic and macroscopic scale.[80] A composite film composed of polyalkylated cyclopentane (MAC) and rGO was prepared on a silicon substrate. The rGO sheets were covalently assembled onto the silicon surface by multilayer deposition. The MAC/rGO composite film had good load carrying capacity, and anti-blocking and anti-wear properties.[81] This strategy can be applied to many other surfaces by simply changing the rGO component.

3.2.2 Amine-functionalized graphene. Lubricants not only need to reduce the friction of mechanical sliding contacts, but also have the task of preventing corrosion. For many lubricants, amines are the basic material. The combination of amine and GO exhibits good performance in terms of solid lubricating and liquid lubricating additives. A common technique for assembling solid lubricants is layer-by-layer assembly, where the coefficient of friction can vary. The utilization of carboxylic acid functionalities present in carbon nanoparticles provides a direct route for covalent functionalization with amine *via* the formation of an amide. The reaction proceeds easily, and the resulting amide functionality is more resistant to hydrolysis than the ester function because the NHR moiety is even a poorer leaving group than OR.

A small number of GO quantum dots functionalized by the covalent bond of the dodecylamine edge was stable up to 220 °C. The modified GO nanocomposite exhibited excellent solubility in various organic solvents. Rapid spraying of the composite onto a steel surface not only reduced the coefficient of friction from 0.17 to 0.11, but also resulted in significant corrosion inhibition.[82] A polytriazine-functionalized rGO (PTZ@rGO) nanocomposite having a terminal amine was obtained *via* a one-step precipitation polymerization method. PTZ@rGO hybrid nanocomposites were selected as fillers to improve the mechanical and tribological properties of BMI resins. As shown in Fig. 6, when the PTZ@rGO content was 0.4 wt%, the composite had the highest flexural strength and 26.5% with the pure BMI resin. When the PTZ@rGO content was 0.6 wt%, the composite had the highest impact strength, the smallest friction coefficient and the lowest volume wear rate. Compared with pure BMI resin, it increased by 46.3%, reduced by 42.9% and decreased by 89.2%.[83] Zhang *et al.* synthesized a novel hydrotalcite film on TC4 titanium alloy *via* a simple hydrothermal method and modified it with graphene and oleylamine.[84] The oleoresin/graphene modified hydrotalcite-based film (HT-OAm/GN) showed a lower friction coefficient. An increased service life and wear performance were observed due to the synergistic effect of the hard and lubricated graphene layer and the oleylamine molecule. Using the UMT-2 tribotester to investigate the tribological properties of nanolubricants dispersed with dodecylamine-functionalized graphene (DAG). The nanolubricants were observed to reduce the coefficient of friction (COF) by a maximum of ~40% in comparison to base engine oil.[85]

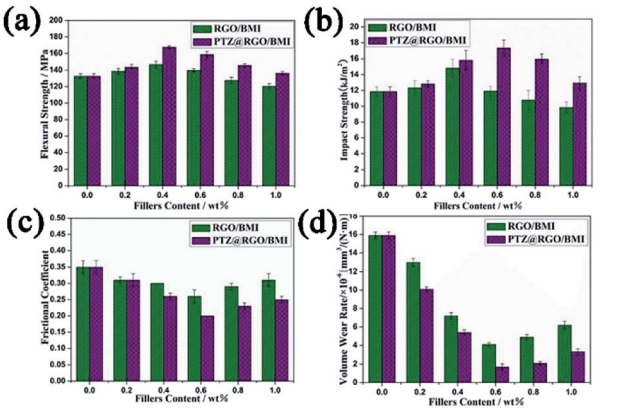

Fig. 6 Relationship between mechanical properties, tribological properties and filler content, (a) flexural strength, (b) impact strength, (c) average friction coefficient, and (d) volume wear rate. Reproduced from ref. 83 with permission from Elsevier, Copyright 2019.

3.2.3 Ionic liquid functionalized graphene. Ionic liquids (ILs) are a new type of green material, which consist entirely of anions and cations and is liquid at room temperature. It has many excellent properties, such as low melting point, non-volatile, non-flammable, and good chemical stability.[86] In addition, it also has good lubricity and electrical conductivity. Based on this, studying the lubrication characteristics of ionic liquids has certain theoretical and engineering significance for improving the friction and wear behavior of materials.

There is a synergistic effect between IL and GO as oil additives, which can reduce friction and enhance wear resistance. Fan *et al.* used an electrochemical method to strip graphene sheets in an ionic liquid solution to prepare a self-assembled ionic liquid graphene sheet multilayer sandwich structure.[87] The self-assembled multilayer graphene (MLG) exhibited a high density of functional group coverage. As a new lubricant additive, the friction coefficient and wear amount were reduced by 55.9% and 84.2%, respectively, at 200 N and 150 °C compared to pure IL. This is due to the synergy of ILs and MLG, because ILs with functionalized MLG can form thin films and tribochemical reaction films on the friction surface during physical adsorption of friction. An IL *in situ*-functionalized GO was uniformly dispersed in epoxy resin (EP) *via* a two-phase extraction route. The IL-functionalized GO (GO–IL) showed significantly improved dispersibility in the EP matrix. At a low load, GO–IL significantly reduced the friction and wear of EP under the entire lubrication state, while the stripped GO nanosheets played an active role under moderate lubrication conditions. Especially under severe friction conditions, there was a significant synergy between IL and GO.[88]

3.2.4 Surfactant-functionalized graphene. Surfactants have a fixed hydrophilic–lipophilic group, which is oriented on the surface of a solution. According to their structure, the commonly used surfactants are classified into ionic surfactants (including cationic surfactants and anionic surfactants), nonionic surfactants, and amphoteric surfactants. Surfactants have proven to be useful additives for the dispersion of carbon

nanomaterials. For example, our research team demonstrated the synthesis of a covalently modified triethanolamine-GO (TMGO) complex *via* a simple hydrothermal method, which was capable of forming a uniform and stable dispersion in water.[89] The micro-morphology of the tribological experiments showed that the friction coefficient and the wear spot diameter of the lubricant-containing TMGO were small, and the optimum tribological properties were exhibited when the content of TMGO was 0.3 wt%. Jia *et al.* reported the friction and wear behavior of oleic acid (OA)-functionalized GO.[90] An OA-functionalized calcium borate/GO (CB/GO) composite was synthesized *via* a hydrothermal method using oleic acid, borax, calcium nitrate and GO. CB decomposed into calcium oxide and boron oxide during the rubbing process, thereby improving the tribological properties. The GO in the composite layer was layered under the action of the transverse frictional shear force and adsorbed on the surface of the friction pair to prevent direct contact. Sodium dodecylbenzene sulfonate (SDBS) was mixed with GO and chemically reduced to obtain graphene. Graphene was stably dispersed in water for three months. SDBS was arranged on the graphene surface by hydrophobic adsorption, which made the graphene hydrophilic, and the electrostatic repulsion between the SDBS anions stabilized the graphene sheet.[91] Under mild conditions, cetyltrimethylammonium bromide (CTAB)-functionalized graphene was prepared by mixing a PVP-stabilized graphene suspension with a CTAB solution under ultrasonic action.[92] Functionalized graphene has better dispersibility in aqueous solution, which provides a good application prospect for its use as a lubricating additive.

3.3 Graphene–polymer nanocomposites

Recently, graphene/GO–polymer materials have attracted great interest due to their high performance even at low filler contents. The properties of graphene–polymer composites depend on the dispersibility of the filler, the adhesion of the filler to the matrix, the ratio of filler to matrix, and the quality of the graphene filler and polymer matrix. The increase in performance is due to the high aspect ratio of the nanofiller, high surface area, and excellent electrical, thermal and mechanical properties. In this chapter, some graphene–polymer nanocomposites are discussed in the field of tribology from the perspective of carbon chain polymers and heterochain polymers.

3.3.1 Carbon chain polymer–graphene nanocomposites. A polymer in which the main chain is completely composed of carbon atoms is usually classified as a carbon chain polymer. Most of the olefinic and diene polymers fall into this category. This section focuses on the use of graphene and GO as fillers in different carbon chain polymer matrices, such as polyethylene (PE), polyvinylidene fluoride (PVDF), polypropylene (PP), polyvinyl alcohol (PVA), polyvinyl chloride (PVC), polytetrafluoroethylene (PTFE), polystyrene (PS), polyacrylate, and polyacrylonitrile (PAN).

A GO/ultra-high molecular weight polyethylene (UHMWPE) composite was successfully prepared by optimizing toluene-assisted mixing followed by hot pressing.[93] When the content of GO nanosheets reached 1.0 wt%, the hardness and wear resistance of the composites significantly improved, and the friction coefficient slightly increased. The main reason for this is that the addition of GO transformed the wear form of UHMWPE from fatigue wear into abrasive wear containing a GO transfer film, which reduced the wear rate of the material. Dimitrios *et al.* prepared a PP composite with graphene added using a melt mixing procedure and evaluated the mechanical properties of the material by tensile testing.[94] It was found that the Young's modulus of the composite was high, there was good interfacial stress transfer between the PP matrix and graphene, and the thermal conductivity of the composite containing graphene was significantly higher. A multilayer graphene (MLG)-filled PVC composite was prepared *via* conventional melt mixing. The presence of MLG can greatly reduce the friction coefficient and wear rate of MLG/PVC composites.[95] PTFE is one of the widely used solid lubricants, but its wear rate is high. When graphene was added to PTFE, it was found that the steady-state wear rate of the composite was reduced by four orders of magnitude.[96] Graphene-wrapping composites are a type of graphene-based composite, which exhibit some potential merits for tribological application. Li's group proposed a highly flexible technique for the manufacture of encapsulated rGO/PVDF composites in solution.[97] The mechanism of successful integration was revealed by electron microscopy. Tribological experiments showed that rGO/PVDF nanocomposites exhibited the best lubricity in all samples (Fig. 7), and the average friction coefficient and wear rate were 44.4% and 98.7% lower than that of paraffin oil.

In addition to the above simple olefin polymers, the preparation and application of some branched olefin polymers and graphene composites have also been studied intensively. GO nanosheets were functionally reduced by *N*-[3-(trimethoxysilyl) propyl]ethylenediamine and then dispersed in polyacrylonitrile to prepare rGO/PAN nanocomposites. The rGO/PAN composite was found to have a suitable rGO loading rate, showing high load carrying capacity and durability.[98] Kumar *et al.* prepared nanocomposites of GO and polyacrylates having 10–18 different carbon atoms by surface-initiated atom transfer radical polymerization (SI-ATRP).[99] The dispersibility of these nanocomposites in an oil medium depended on the graft density of the polyacrylate on the surface of the graphene, and the degree of dispersion and stability increased as the chain length increased. The optimized loading was 0.04 mg mL^{-1} GO/C18-

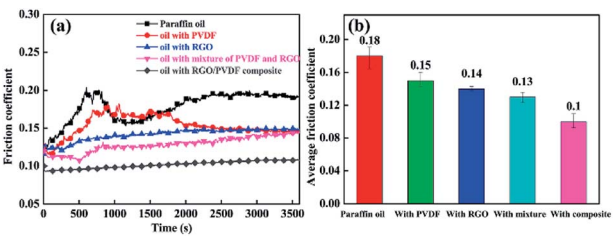

Fig. 7 (a) Friction coefficient and (b) average friction coefficient under five different lubrication states. Reproduced from ref. 97 with permission from Elsevier, Copyright 2018.

polyacrylate nanocomposites in base oils and polyols, significantly reducing friction and wear by about 42% and 34%, respectively, and improving the friction and wear properties, thereby improving the tribological performance. Shi *et al.* prepared a GO-containing PVA (PVA/GO) composite *via* a freeze-thaw method, and irradiated it with different doses of gamma rays to improve its strength and wear resistance.[100] Gamma ray irradiation can promote the binding of GO nanosheets to PVA in the form of covalent bonds. The resulting composite had high strength and improved thermal stability. Also, the wear resistance was significantly improved during the irradiation treatment. The composite materials had high strength and improved thermal stability. Also, the wear resistance was remarkably improved during the irradiation treatment.

The addition of graphene to a diene-based polymer also significantly improved its tribological properties.[101] For example, Li *et al.* prepared GO/nitrile rubber (NBR) nanocomposites having various GO contents by solution mixing. The tribological properties of GO/NBR nanocomposites were completely different under different tribological conditions. In the dry friction state, since GO can be easily transferred from the substrate to the mating surface to form a continuous and compact transfer film, and the coefficient of friction (COF) and specific wear rate of the nanocomposite decreased. Under water lubrication conditions, due to the formation of strong hydrogen bonds between GO and water molecules, a thicker water film was formed between the composite materials, and the COF and specific wear rate significantly increased. The poor dispersibility of graphene in a non-polar polymer matrix limits the application of graphene to some extent. Wu *et al.* grafted PS or poly(-styrene-*co*-isoprene) (PSI) onto the surface of GO, which improved the dispersibility of graphene in a solution of styrene butadiene (SSBR) and butadiene rubber (BR).[102] Also, the improved dispersibility of GO in SSBR–BR composites significantly ameliorated tensile strength and wear resistance compared to that of the pure SSBR–BR composites under a low load.

3.3.2 Heterochain polymer–graphene nanocomposites. In addition to carbon atoms, heterochain polymer macromolecular chains have hetero atoms such as oxygen, nitrogen and sulfur. The tribological properties of graphene nanocomposites prepared from five different classes of heterochain polymers are described below.

(1) Polyether-type

Polyetheretherketone (PEEK) is a common thermoplastic in the industrial and biomedical fields. PEEK with graphene nanosheets (GNP) was prepared by solvent-less melt blending and injection molding. Studying the tribological properties of the composite, it was found that the hardness of the composite surface significantly improved (60%), the friction coefficient was reduced (38%), and the wear coefficient was greatly reduced (83%).[103] GNP was used as a filler in PEEK-based materials without any chemical functionalization, improving their surface hardness and tribological properties. Wang *et al.* successfully prepared a three-layer film consisting of GO and perfluoropolyether (PFPE) on a silicon substrate pre-modified with self-assembled 3-aminopropyltriethoxysilane (abbreviated as APS–GO/PFPE).[104] Compared with unmodified ordinary perfluoropolyether film, the APS–GO/PFPE film had better anti-friction and wear resistance, which was attributed to the excellent wear resistance of GO and excellent lubricity and low shear strength of PFPE. Pan *et al.* used an oxidation–dispersion–reduction method to prepare polyphenylene sulfide (PPS)/polytetrafluoro wax/graphene composite coatings.[105] The tribological performance test results showed that the friction coefficient of the composite coating was lower than that of the pure PPS coating, and the wear life was significantly higher than that of the pure PPS coating. The wear form of the pure PPS coating was severe adhesive wear, while the composite coating was dominated by abrasive wear, and the dual ring of the composite coating formed a uniform and tough transfer film.

(2) Polyester-type

A new class of polyester nanocomposites with GO was obtained *via* a specific chemical method.[106] Through the wear test of the nanocomposite block on the steel ring, it was concluded that the incorporation of GO nanosheets into the polyester matrix at very low levels resulted in significantly altered tribological properties. The inclusion of GO in the polyester matrix resulted in better anti-wear behavior of the nanocomposite. Lei *et al.* prepared GO/unsaturated polyester (GO/UP) composites by *in situ* polymerization.[107] The effects of GO content on mechanical properties, hardness, friction and wear properties and electrical properties of composites were investigated. When the GO content was 0.50%, the impact strength of the composite increased by 14.69%; when the GO content was 0.25%, the flexural strength of the composite increased by 13.89%; and when the GO content was 0.75%, the volume wear rate of GO/UP composite was reduced by 54.7%.

(3) Polyamide homologs

Pan *et al.* prepared a polycaprolactam (PCL)-adapted nanocomposite containing porous graphene (PG) impregnated with solid paraffin *via in situ* polymerization.[108] When the PG content was 10%, the PCL/PG composite exhibited the minimum friction coefficient and wear rate. Also, as the pressure and friction velocity increased, the friction coefficient and wear rate of the composite became lower and more stable than that of pure PCL. This was due to the formation of a suitable surface film under high load conditions of the graphene nanosheets, and the friction heating caused the paraffin to melt to produce a lubricating effect at the sliding interface. Simultaneously, it also eliminated the frictional heat to avoid thermal damage to the surface. Min's group synthesized a polyimide (PI)/GO nanocomposite film *via in situ* polymerization.[109] PI/GO exhibited better tribological properties under seawater lubrication conditions than other conditions. The wear resistance of GO was greatly improved by filling GO under seawater lubrication, and the wear resistance of PI reached a peak when the GO content was 0.5 wt%. Because of the strong interfacial adhesion between the PI matrix and the GO nanofiller, the load could be effectively transferred between the contact faces.

(4) Polyurethane

Polyurethane (PU) materials have excellent wear resistance, corrosion resistance, flexibility and strong adhesion to matrix materials. However, conventional PU materials have some

inherent disadvantages, such as poor thermal stability, low stiffness, and low tensile strength. Thus, to improve its mechanical durability, it is necessary to modify the polyurethane to improve its tribology and corrosion resistance. Mo's team produced functionalized graphene (FG) and functionalized graphene oxide (FGO) reinforced PU composite coatings with different concentration gradients.[110] The dispersibility and compatibility of graphene and GO were improved by chemical modification. The tribological properties of the two composites showed the same trend. With an increase in the FG or FGO content, the friction coefficient and wear rate of the two composites increased first and then decreased. When the FG content was 0.25 wt% and the FGO content was 0.5 wt%, the tribological properties of the two composites were optimized respectively. By tribological experiments in a seawater environment, it was found that the FGO/PU coating exhibited better tribological properties than the FG/PU coating. However, since the oxidation group of FGO/PU was rich, the corrosion resistance was worse.

(5) Resin

Epoxy resin (EP), as an important thermosetting matrix for advanced engineering composites, has the advantages of high hardness, low solid shrinkage, strong chemical resistance and good dimensional stability. However, pure epoxy resin has high brittleness and poor wear resistance after curing. Thus, for its development in engineering applications, it is imperative to fill and modify it. Shen *et al.* studied the tribological properties of GO/epoxy nanocomposites.[111] The wear resistance was remarkably improved by adding GO to the epoxy resin. Also, when the GO content was equal to 0.5 wt%, the specific wear rate with respect to the pure epoxy resin was lowered by 90.0–94.1%. GO nanosheets have a high specific surface area and their corrugated surface adheres well to epoxy resin. Li's group first obtained a solventless GO nanobelt colloid (GONRs-M2070) by grafting organosilane (KH560) and polyetheramine (M2070). An epoxy composite was then prepared from the GONRs-M2070 colloid based on the *in situ* blending method.[112] GONRs-M2070 can be well dispersed and stripped in EP. Experiments were carried out on epoxy composites with different contents of GONRs-M2070. As shown in Fig. 8, the addition of GONRs-M2070 can enhance the mechanical properties of EP, and when the GONRs-M2070 content was 0.6 wt%, the flexural strength and impact strength of the epoxy composite material reached a maximum. On the other hand, the friction coefficient and wear rate of the epoxy composites were much lower than that of pure EP. Also when the content of GONRs-M2070 was 0.6 wt%, the epoxy composite exhibited the optimum tribological properties.

In addition to epoxy resins, the tribological properties of phenolic resins and cyanate resins with graphene or GO prepared as nanocomposites have also been investigated. Poly(phenolic resin)/carbon fiber composite materials having different ratios of graphene–Fe_3O_4 were prepared *via* a molding method. Fe_3O_4 was introduced into graphene to avoid recombination of the layers. Based on tribological results, the friction coefficient and wear rate were reduced after the addition of graphene–Fe_3O_4.[113] Lin *et al.* prepared a GO nanosheet (GONS)/cyanate ester (CE) resin composite *via* a solution intercalation method.[114] A tribological system and thermogravimetric analysis (TGA) were used to characterize the tribological properties and thermal stability of the GONSs/CE resin composites, respectively. The results showed that the addition of GONS improved the mechanical and tribological properties of CE resin. Also, the composite exhibited better thermal stability than the CE resin matrix.

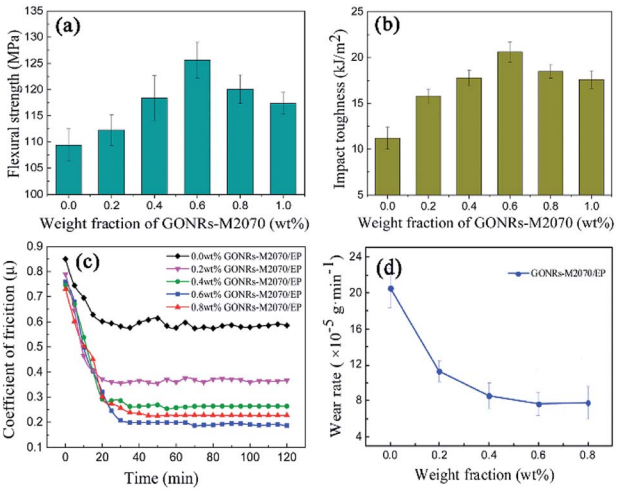

Fig. 8 (a) Flexural strength, (b) impact strength, (c) friction coefficient and (d) wear rate of GONRs-M2070/EP composites with different weight fractions of GONRs-M2070. Reproduced from ref. 112 with permission from Elsevier, Copyright 2016.

4 Ultra-low friction and superlubricity

In the past two decades, significant progress has been made in experimental research and theoretical analysis of ultra-low friction and superlubricity. Graphene-based materials have long been studied as excellent lubricants, and the superlubricity of graphene has been reported experimentally and theoretically.[115–117] The following is the research status of graphene-based materials from two aspects, ultra-low friction and superlubricity.

4.1 Ultra-low friction of graphene-based nanocomposites

Amorphous carbon (a-C) films have good research prospects as solid lubricant coatings. They significantly reduce friction and relieve wear, thereby increasing the service life of friction pairs. Gong *et al.* synthesized hydrogenated a-C films *via* plasma enhanced chemical vapor deposition (PECVD).[118] They monitored the structural evolution of the friction film and the decrease in friction coefficient. Finally, the growth model of graphene nano scrolls (GNSs) and the friction mechanism transformation of the a-C materials were revealed, as shown in Fig. 9. In the initial stage of friction, the non-equilibrium carbon atoms were converted to graphene under the action of shear stress and frictional heat. Due to the spontaneous decrease in surface energy, the graphene sheets tended to wrap amorphous carbon or smaller GNS to reduce the surface area. When the friction process tended to reach equilibrium, under

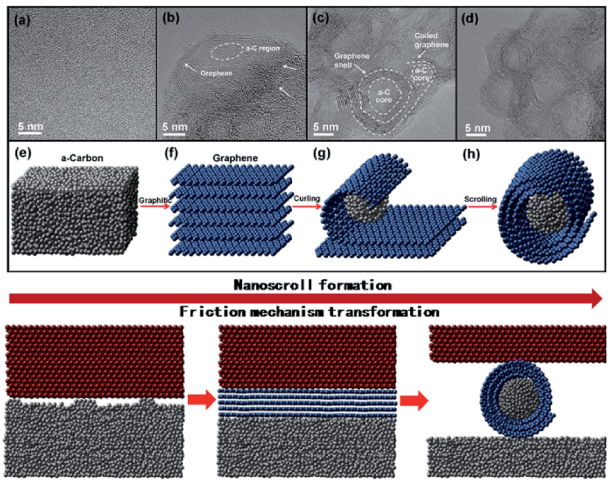

Fig. 9 (a) HRTEM images of a-C films. Tribofilm after (b) 200, (c) 1000 and (d) 7500 cycles of friction at 10 N and 10 Hz. Schematic diagram of graphene formation during friction (e)–(h). The bottom shows the mechanism diagram of the interface friction mechanism transition. Reproduced from ref. 118 with permission from Elsevier, Copyright 2017.

the action of shear stress, adhesion recombination occurred at the interface, eventually leading to the formation of a large class of GNS. As the GNS polymerized, the coefficient of friction decreased accordingly. Therefore, this phenomenon indicated the ultra-low friction new friction mechanism of the a-C film. When the hard material slides relative to the soft material, the soft material peels off and transfers to the surface of the hard material to form a film to reduce friction. Saravanan's team demonstrated that a multilayer polyethyleneimine/GO film (PEI/GO) exhibits superlubricity on steel surfaces.[119] Subsequently, they studied the COF and wear of PEI/GO with six different polymer spheres sliding in air and nitrogen, with particular attention on the formation of friction transfer membranes in this process.[120] The six polymers were polyoxymethylene (POM), PEEK, PE, poly(methyl methacrylate) (PMMA), polycarbonate (PC) and PTFE. It was found that in nitrogen, four polymers (POM, PEEK, PMMA and PC) showed ultra-low friction, while the other two did not (PTFE and PE). The tribological behavior was related to the hydrophilicity and relative hardness of the polymer sphere. Wang *et al.* designed a self-assembling friction device with a single structural film coated on both sliding surfaces and collecting the converted product under different loads and slip cycles.[121] This film was a carbon-based film composed of sp^2-rich carbon. An ultra-low friction (0.005) could be achieved by low shear strength graphene formed at the graphite-like carbon (GLC) interface during the rubbing process. Also, to achieve ultra-low friction (0.009), reduce the contact area by spherical nanoparticles with an outer graphite shell produced at the fullerene-like carbon (FLC) interface.

4.2 Superlubricity of graphene-based nanocomposites

Ultra lubricity is a subject that has attracted wide interest in the field of tribology. Depending on the state of lubricants, they are usually classified into solid superlubricity and liquid superlubricity.[122] Due to different application fields, the preparation method and lubrication mechanism are also different. Graphene-based materials have proven to be ideal candidates for superlubricity due to their excellent self-lubricity.

When graphene forms a disproportionate contact at low contact pressures, the superlubricity of graphite and graphene slipping can be easily achieved at the nanoscale. However, achieving ultra-lubricity under ultra-high contact pressure (>1 GPa) so that graphene can have more applications in the lubrication of micro-mechanical and nano-machines still needs in-depth study. Li *et al.* prepared graphene by stripping highly ordered pyrolytic graphite (HOPG).[123] The graphene film was transferred to the AFM probe tip for tribological experiments and found to achieve a friction coefficient as low as 0.0003 at ultra-high contact pressures of up to 2.52 GPa. Characterization found that the extremely low shear strength of the graphene/graphite interface in disproportionate contact caused the occurrence of graphene superlubricity. Moreover, the superlubricity of graphene to graphene was stable under ultra-high contact pressure, which can also accelerate its application in nano-scale lubrication. In addition to obtaining tribological data on graphite and graphene by sliding the tip of the AFM, the origin of superlubricity was investigated. The superlubricity of graphene materials can also be explored by the relative motion between graphene layers. Using scanning tunneling microscopy, Feng *et al.* found that graphene nanoflakes (GNFs) showed easy translational and rotational motion between the respective initial and final states at temperatures as low as 5 K.[124] This movement began with the tip-induced sheet changing from a corresponding registry to a disproportionate registry. With the graphene layer below (superlubric state), it then slid quickly until another commensurate position was reached.

Graphene and other two-dimensional materials have been shown to achieve ultra-lubrication under specific application conditions. Wang *et al.* prepared single-layer graphene and MoS_2 nanosheets by mechanical lift-off.[125] A non-destructive transfer was then performed to transfer the single layer of graphene to a single layer of MoS_2. Thereby, an assembled van der Waals heterostructure was prepared. Through density functional theory calculation and Raman spectroscopy, the shear force constant between the formed graphene/MoS_2 heterojunction layers was reduced by two orders of magnitude, which could achieve the conventional superlubricity. This work provides a new perspective for understanding atomic-scale friction and superlubricity. Stable superlubricity can be achieved by assembling different materials to obtain a van der Waals heterostructures. Mandelli *et al.* used molecular dynamics to study the nanoscale tribological properties of graphene/graphene homogenous materials and graphene/h-BN heterojunction materials.[126] As shown in Fig. 10, when two layers of nanosheets were aligned ($\theta = 0°$), the homogeneous material produced a size-independent static and kinetic coefficient of friction. Heterojunction materials exhibited tribological phenomena from stick-slip motion to smooth motion to ultra-lubrication. When the two materials were chosen to be small (2.4 nm^2) and rotated to $\theta = 30°$, the homogenous materials

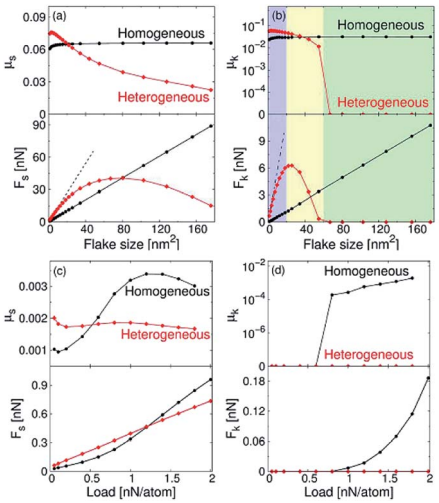

Fig. 10 Variation in (a) static friction coefficient (μ_s) and force (F_s) and (b) kinetic friction coefficient (μ_k) and force (F_k) with flake size under a load of 0.1 nN per atom. Variation in (c) μ_s and F_s and (d) μ_k and F_k with load for a flake size of 2.4 nm^2. Reproduced from ref. 126 with permission from Nature, Copyright 2017.

could achieve superlubricity only at lower experimental forces. The heterojunction material still exhibited superlubricity behavior under higher load forces. As a result of these experiments, layered heterojunction materials with a certain mismatch angle have become candidates for new superlubricity materials.

Superlubricity can be achieved on the nano or micron scale of two-dimensional layered materials such as graphite, boron nitride and molybdenum disulfide by forming the desired disproportionate contact. However, due to size limitations, the contact area has never been observed on a macroscopic scale. Li *et al.* performed a tribological experiment on a substrate made of HOPG using a universal macro-tribotester.[127] It was found that a plurality of frictionally transferred multilayer graphene nanoflakes (MGNF) were formed on the steel contact zone after the initial sliding, and the instantaneous superlubricity of graphite to steel was realized on a macroscopic scale. As shown in Fig. 11, the minimum friction coefficient was as low as 0.001 at 404.8–407.2 s and the maximum sliding distance was 131 mm. This indicated that the instantaneous superlubricity of graphene sliding on steel can be achieved randomly on a macroscale. This macroscopic superlubricity mechanism can be attributed to the weak interaction between the layered materials

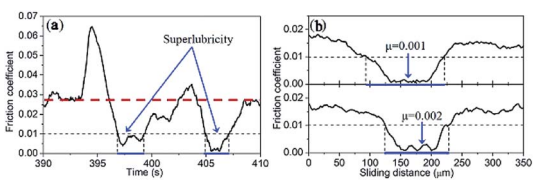

Fig. 11 (a) Friction coefficient changes with time and (b) friction coefficient changes with sliding distance. Reproduced from ref. 127 with permission from Elsevier, Copyright 2018.

and the formation of transfer films during the lubrication process. Although graphene is recognized as an excellent lubricating material due to its two-dimensional structure and weak interlayer interaction, most research involving the superlubricity of GO has been limited to the nanoscale or micron size (about 1–10 μm). Ge *et al.* used the synergistic effect of graphene-oxide nanosheets (GONF) and ethylene glycol (EDO) at the Si_3N_4–SiO_2 interface to achieve a robust macroscopic super-lubrication state (μ = 0.0037).[128] It was observed that GONF was adsorbed on the surface of the friction pair to prevent direct contact. Due to the presence of GONF and EDO between the contact interfaces, extremely low shear forces were produced, which contributed to improve the superlubricity for ultra-low wear. Simultaneously, the formation of a hydrated GONFs–EDO network by hydrogen bonding interactions at the GONFs–EDO interface contributed to the extremely low shear stress of the liquid lubricating film.

5 Applications

Since the development of graphene-based nanocomposites in tribology and lubrication applications, the physical and mechanical properties of graphene-based materials have shown many potentials and unique features to improve many applications related to lubrication performance. Significant research has been devoted to the potential lubrication mechanism of graphene as a lubricant, which can serve as guiding applications. In this chapter, we first review the lubrication mechanism of graphene materials as nano-lubricants, and then propose several applications including micro-tribology applications, bio-tribology and lubrication applications, and industrial lubrication applications.

5.1 The mechanism of graphene nano lubricants

At present, research shows that graphene as a two-dimensional nano-lubricant plays the main role in the anti-friction and anti-wear effect by: (1) entering the friction pair contact zone, (2) forming a friction film and a transfer film, and (3) adsorbing on the friction pair surface peaks and valleys.

(1) Entering the friction pair contact zone

The graphene material has a two-dimensional sheet structure that allows it to easily enter the frictional contact area. Graphene nanocomposites functionalized by covalent or non-covalent bonds have surface-grafted nanoparticles that can further enhance their ability to enter the frictional contact zone.[129] When graphene materials are involved in lubrication, they are subjected to normal load forces. Simultaneously, the relative motion of the two contact surfaces produces shear forces. The layered graphene material is easily sheared and can be effectively involved in lubrication.[130]

(2) Forming a friction film and a transfer film

In the liquid lubrication process, the friction film and the transfer film are formed at the contact area of the sliding surface. At the beginning of the friction, the high surface energy and shear properties of the graphene nanocomposites make them easily adsorbed onto the surface of the friction pair to

form a physical protective film. As the friction progresses, the flake graphene material is worn into a small-diameter graphene material under the action of contact secondary friction. This material has a smaller sheet diameter, an increased degree of defects, and is easily transferred with the flow of the lubricant to deposit in a region not covered by graphene.[131] The presence of the transfer film facilitates the formation of the integrity and continuity of the protective film on the surface of the friction pair. The primary purpose of physical and transfer films is to prevent direct contact between two sliding surfaces and to reduce friction and wear. When the bearing capacity is large or the sliding time is too long, the physical film will rupture, thereby generating a large amount of heat and stimulating a frictional chemical reaction between the lubricating additive and the surface of the friction pair to form a chemical reaction film.[132] The presence of a chemically reactive film greatly improves the tribological properties of the lubricant.

(3) Adsorbing on the friction pair surface peaks and valleys

Since the surface of the friction pair forms a rugged gully during the rubbing process. The presence of roughness creates a high contact pressure during the rubbing process. Two-dimensional graphene materials, especially functionalized modified graphene nanocomposites, can not only fill the concave area on the surface, but also adsorb on the peak of the roughness,[133] thereby reducing the friction between the friction surfaces during the rubbing process. In addition, the graphene material in the recessed regions and on the peaks contributes to the formation of a continuous oil film, thereby further enhancing lubricity.[134]

5.2 Micro-tribology applications

With the continuous penetration and rapid development of microelectronics in various fields, the development of machinery on the micro-small scale has been greatly promoted, and small engineering structures called MEMS and nano-electromechanical systems (MEMS and NEMS) have been developed. Due to the reduction in size in this system, the gap size of the friction pair is often in the nanometer or even zero gap. The friction effect is very prominent due to the size effect during the motion, which becomes a key factor affecting the performance of MEMS and NEMS. In this system, which is essentially in the field of micro-tribology, the actual contact area consisting of small contact roughness peaks makes up a small portion of the apparent contact area.

Li *et al.* prepared an rGO nanofilm on a deposited Ti substrate or a self-assembled monolayer (SAM) of a 3-amino-propyltriethoxysilane (APTES)-modified surface of a Ti alloy substrate.[135] The nanoscale tribological behavior of AFM and UMT-2 microscale was studied to provide a basis for improving the surface properties of titanium materials in bioMEMS or NEMS. The Ti substrate, APTES SAM and GO–APTES nanolayers were compared in a nano-friction test. The results showed that the rGO–APTES nanolayer had excellent tribological properties. In the micro-friction test, the nanolayer of rGO–APTES on the Ti substrate exhibited a low COF (0.16) and an long anti-wear life (10 000 s). To reduce the friction between graphene and the tip of AFM, Zeng *et al.* created a stronger van der Waals attraction between graphene and the substrate by plasma treatment, and enhanced the adhesion of graphene to the base.[136] The enhanced van der Waals attraction reduced the friction of graphene, and the effect of the reduction was independent of the thickness of the graphene nanosheets and the type of AFM tip. It was also found that the longer the plasma treatment time, the stronger the adhesive attraction and the smaller the friction. This study plays a key role in graphene-coated MEMS/NEMS systems. The attraction of graphene and its deposition substrate was enhanced by a convenient and low-cost method, the friction between the micro-mechanical components was reduced, and the reliability and stability of the system were improved. The epoxy and hydroxyl groups present on the GO sheet were converted into carboxyl groups by sonicating a mixture of GO and chloroacetic acid. The carboxyl-GO sheet was assembled on a silicon substrate using 3-amino-propyltriethoxysilane (APS) as an intermediate coupling agent (labeled APS–GO). An La element was deposited on APS–GO by chemisorption to form a multilayer film (APS–GO–La). The experimental results showed that the carboxyl-GO sheets were uniformly distributed on the Si substrate, and the prepared APS–GO–La multilayer film exhibited low surface free energy and excellent micro-tribological properties in N/MEMS.[137]

Robinson's group studied the dependence of micro-friction on the local environment in microfluidics and MEMS and nanoelectromechanical systems. The different surrounding media were air, polar (water) and non-polar (dodecane) liquid. The coefficient of friction in the liquid was significantly reduced, but the graphene in the non-polar dodecane was higher than the polar water. Further research found that ultrasonic vibration can reduce the friction between running parts in a fully immersed system, providing a new way to eliminate the friction between NEMS and nanostructures operating in a liquid environment.[138] Ultra-low friction and wear in micro/nanoscales in micromechanical systems, including MEMS, delivered superior performances and long-lasting operation. Traditional solid lubricants offer low friction only in micro/macroscale wet environments and are not suitable for practical microscale applications. AFM measurements showed that multilayer graphene films have superior nanoscale friction properties. Regardless of the corresponding AFM tip material, their friction is significantly lower than that achieved with conventional lubricants.[139] In particular, the ultra-low friction of single-layer graphene that realizes CVD growth on silicon dioxide makes its application in micromechanical systems more powerful.

5.3 Bio-tribology and lubrication applications

There are a large number of tribological phenomena in living things, especially humans, such as teeth, bones, skin, *etc.*, revealing the extensiveness of tribology in the human body, and thus it is of great significance to manufacture artificial biological materials to replace human biological materials. In particular, articular cartilage has a low wear and friction for up to 70 years. In the case of accidental injury, self-repair is very difficult,

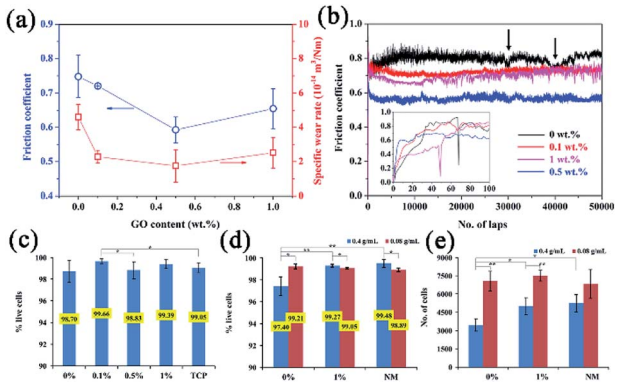

Fig. 12 Variation in (a) friction coefficient, specific wear rate and (b) friction coefficient cures with GO content. (c) Viability of MG63 cells after 72 h culture on GNP/45S5 composites and tissue culture plastic. (d) Viability and (e) number of MG63 cells after 72 h culture in pellet leachates and NM. Reproduced from ref. 142 with permission from Elsevier, Copyright 2017.

and it is necessary to introduce artificial materials to achieve its function. Statistics has shown that due to the current aging population and the increase in accidental injuries, the disease of joint damage is also increasing. Therefore, extending the service life of synthetic biomaterials and developing materials with good biocompatibility, low production cost, low friction and wear are one of the important sources for promoting the development of biomedical materials.

Xu *et al.* successfully prepared a new type of artificial joint replacement material, a fluorinated graphene (FG)/UHMWPE composite, by ultrasonic dispersion and liquid thermoforming.[140] Through tribological experiments and biosafety experiments, the results showed that the addition of FG to pure UHMWPE not only improved the micro-hardness of the composite, but also significantly reduced the wear of the composite. As the FG content increased, the friction coefficient of the composite material also decreased. Furthermore, MC3T3-E1 cells adhered and grew well on the surface of the FG/UHMWPE composite, indicating that the addition of FG did not affect the morphology and activity of the cells. The excellent mechanical properties, tribological properties and biomedical properties of graphene and its derivatives and graphene-reinforced nanocomposites have attracted great attention from researchers. Dong reviewed the tribological properties, biocompatibility and biosurface engineering of graphene-based materials. Graphene and GO reinforced composites were considered to be ideal for low friction, self-lubricating, highly bioactive and antimicrobial materials on biological surfaces.[141] 45S5 Bioglass (45S5) has excellent biocompatibility and bioactivity and is one of the most widely used biomaterials in ceramic-based bone graft replacement. Four different amounts of GO composite powder, *i.e.*, 0, 0.1, 0.5, and 1 wt%, were loaded onto 45S5 Bioglass by spark plasma sintering (SPS) at 550 °C. When 0.5 wt% of GO was added, the fracture toughness of the sintered pellet of the composite increased by 130.2%, and the friction coefficient and specific wear rate decreased by 21.3% and 62.0%, respectively (Fig. 12).[142] Also, the viability of MG63 cells grown on GNP-containing particles was comparable to cells grown on the pure 45S5 particles. The GNP/45S5 particle-regulated medium made of a composite powder with 1 wt% GO enhanced the proliferation and viability of MG63 cells compared to pure 45S5 leachate.

5.4 Liquid lubrication additives applications

Due to the adverse effects of friction on efficiency, component life and green environmental, reducing friction in mechanical systems and mechanical failures associated with wear has attracted increasing attention. One way to reduce friction and control wear is to use a liquid lubricant. A liquid lubricant reduces friction by forming a low shear on the friction surface, and the high durability boundary film prevents direct contact of the sliding contact interface. The type and performance of additives in liquid lubricants directly affect the lubrication and anti-wear properties of the lubricant. Current research has shown that graphene-based materials can be used as additives in various lubricants, such as oils, organic solvents and other types of fluids, thereby reducing friction and improving lubrication.

The effect of adding graphene to a standard lubricant to produce a high performance compound was investigated. Grease and two lubricants were selected as the base lubricant, and the COF of the graphene compound lubricant with different compositions was evaluated. The experimental results showed that the graphene added to the lubricant generally had a lower coefficient of friction than the original lubricant. The properties of the graphene-added greases were consistent with previous studies of mechanical components (spline coupling), which have been widely used in many industrial scenarios.[143,144] Due to the excellent performance of graphene materials as liquid lubricant additives, researchers are more interested in factors affecting the lubricity of graphene. Studies have shown that many factors such as sheet diameter, interlayer distance, degree of on-chip defects, number of graphene layers, and hardness, all have more or less influence on their lubricating properties. The effects of different microstructures of graphene on the properties of lubricating additives were studied. The lubrication properties of three rGO sheets with different microscopic morphologies were studied. The three rGO sheets were regular edge (RG), irregular edge (ir-RG) and irregular edge and wrinkle (ir-RWG). Tribological experiments showed that RG had the best lubricity, and its use as a lubricating additive significantly reduced the friction coefficient and wear depth to 27.9% and 14.1%, respectively, while ir-RWG exhibited the worst lubrication performance.[145] It is believed that the morphology of graphene sheets directly affects their lubricating properties, and the more regular the morphology, the better the lubrication performance. Mura *et al.* studied the effect of graphene nanosheets as additives in standard greases.[146] The spline coupling was selected as an experimental test solution. This component was subject to great wear during operation, and the reduction of the friction coefficient could reduce the wear problem and improve the efficiency and reliability of the component. The experimental results proved that GNP have great benefits in

reducing COF. Using only 0.5% GNP resulted in a 8.5% reduction in the COF of the grease. When the GNP content was increased to 10%, the COF of the grease was reduced by 16.3%. The addition of graphene promoted the formation of a boundary film of the grease during the rubbing process, thereby improving the lubricating performance. The relationship between the size and tribological properties of GO as an additive in oil was investigated innovatively by using modified Hummers methods to prepare GO nanosheets with different sizes at different oxidation temperatures.[147] As the GO size decreased, the C/O ratio decreased. In the oils containing 0.04 wt% of GO, the GO base oils exhibited excellent friction reduction and anti-wear properties. It was also found that GO nanosheets having a smaller size and a lower C/O ratio acted as lubricating additives to perform more significantly in improving the tribological properties of the oil.

6 Summary and outlook

In summary, various methods have been developed such as electrochemical stripping, self-assembly, simple one-pot hydrothermal method, solvothermal method, co-precipitation and precipitation polymerization, *in situ* carburization, one-step precipitation polymerization and solution intercalation for the preparation of graphene derivatives and their nanocomposites. Graphene-based composites not only fully inherit the excellent mechanical properties and thermal stability of graphene materials, but also have some unique advantages due to the grafting of functional molecules on the surface or edge of the sheet. For example, dispersion is easier, stability is increased, adsorption is enhanced, the shear stress required for interlayer slip is reduced, and the film formation strength is increased. Considering the above advantages, graphene-based nanocomposites have made great breakthroughs in the field of tribology and lubrication.

However, although considerable advances have been made in the laboratory-scale studies on the excellent tribological and lubricity properties of graphene-based nanocomposites, much effort is still needed to promote a wide range of commercial applications of graphene nanocomposites. Future research should be conducted on the following aspects: (1) reducing the preparation cost and synthesizing graphene sheets with controlled size and shape. The usual preparation methods, such as solvothermal method, hydrothermal method, and self-assembly, use concentrated sulfuric acid, nitric acid, concentrated hydrochloric acid and hydrazine hydrate, and the waste liquid generated by the reaction pollutes the environment. Graphene-based materials prepared by substrate-assisted CVD deposition have good quality, but the substrate removal work cost is high, and a large amount of toxic waste liquid is also generated. This is also one of the main reasons for restricting the application of graphene-based nanocomposites in MEMS or NEMS. Therefore, the development of substrates that are easy to remove and do not affect the quality of graphene is of great significance for reducing the cost of graphene preparation and accelerating its application process. (2) Although a large number of studies have confirmed that graphene-based nanocomposites have excellent antifriction, antiwear and lubrication effects, the lubrication mechanisms of the same and different types of graphene-based nanocomposites have not been summarized in detail. For example, when graphene and nano-metals form a composite material to participate in lubrication, what functions do the metal particles and graphene play, and what synergy exists between the two? It is also necessary to understand the above problems in the formation of nanocomposites of graphene and metal sulfides, nitrides, alkyl groups, ionic liquids, surfactants, *etc.* in lubrication. Based on a large number of studies, it can be concluded that the interaction between graphene and different types of functionalized molecules and the role played by lubrication are established. More mature theories may contribute to the functionalization of graphene, the preparation of materials with expected properties, and bring a new direction for the application of graphene nanocomposites in the field of tribology and lubrication. (3) Due to the different tribological states in different application scenarios, the performance of graphene nanocomposites depends on the type and structure of the functionalized molecules, and the physical structure of graphene-based nanocomposites before preparation. Thus, their chemical properties should be simulated and calculated. On the one hand, this facilitates the synthesis of graphene-based nanocomposites with optimized structures, controlled morphology and custom properties. On the other hand, it promotes the application of graphene in the micro–nano field and industrial lubrication additives. Therefore, a new strategy for synthesizing graphene nanocomposites with finely controlled structures is very important.

At the same time, research on the ultra-low friction and superlubricity of graphene-based nanocomposites is emerging. Due to the unique layered structure of graphene and the low van der Waals force between its layers, it easily shows natural superlubricity. Numerous studies have shown that graphene can achieve ultra-low friction at micro–nano levels and at very low pressures. This limits the use of graphene-based nanocomposites in some micron or even nanoscale lubrication systems. Although the three-dimensional multilayer graphene surface composed of single-layer graphene nanosheets can achieve super-lubrication behavior under high load, superlubricity failure eventually occurs due to the significant deformation-by-layer peeling of the graphene sheets.

In summary, although challenges and problems remain, it is clear that graphene-based nanocomposites show very bright and exciting prospects in the field of tribology and lubrication. By continuously improving the preparation methods and techniques, perfecting their antifriction and antiwear mechanism and lubrication mechanism, graphene-based nanocomposites will surely shine in micro–nano friction systems, bio-tribology and industrial lubrication.

Conflicts of interest

There are no conflicts to declare.

Acknowledgements

The work was supported by Beijing Natural Science Foundation (No. 2182041).

Notes and references

1 H. Xiao and S. Liu, *Mater. Des.*, 2017, **135**, 319–332.
2 K. Holmberg, P. Andersson, N. O. Nylund, *et al.*, *Tribol. Int.*, 2014, **78**(4), 94–114.
3 P. Restuccia and M. C. Righi, *Carbon*, 2016, **106**, 118–124.
4 J. Li, X. Zeng, T. Ren, *et al.*, *Lubricants*, 2014, **2**, 137–161.
5 J. C. Spear, B. W. Ewers, J. D. Batteas, *et al.*, *Nano Today*, 2015, **10**, 301–314.
6 H. Yu, Y. Xu, P. Shi, *et al.*, *Surf. Coat. Technol.*, 2008, **203**, 28–34.
7 R. Raccichini, A. Varzi, S. Passerini, *et al.*, *Nat. Mater.*, 2015, **14**, 271–279.
8 W. Peng, H. Li, Y. Liu, *et al.*, *J. Mol. Liq.*, 2017, **230**, 496–504.
9 R. Narayan, J. E. Kim, J. Y. Kim, *et al.*, *Adv. Mater.*, 2016, **28**, 3045–3068.
10 J. S. Choi, J. S. Kim, I. S. Byun, *et al.*, *Science*, 2011, **333**, 607–610.
11 A. Klemenz, L. Pastewka, S. G. Balakrishna, *et al.*, *Nano Lett.*, 2014, **14**(12), 7145–7152.
12 M. Tripathi, F. Awaja, G. Paolicelli, *et al.*, *Nanoscale*, 2016, **8**, 6646–6658.
13 D. Berman, A. Erdemir, A. V. Sumant, *et al.*, *Mater. Today*, 2014, **17**, 31–42.
14 J. Yang, Y. Xia, H. Song, *et al.*, *Tribol. Int.*, 2017, **105**, 118–124.
15 S. Park, J. An, I. Jung, *et al.*, *Nano Lett.*, 2009, **9**(4), 1593–1597.
16 A. D. Moghadam, E. Omrani, P. L. Menezes, *et al.*, *Composites, Part B*, 2015, **77**, 402–420.
17 H. Song, B. Wang, Q. Zhou, *et al.*, *Appl. Surf. Sci.*, 2017, **419**, 24–34.
18 Z. Xu, Q. Zhang, W. Zhai, *et al.*, *RSC Adv.*, 2015, **5**(113), 93554–93562.
19 P. Wang, W. Zhang, D. Diao, *et al.*, *Surf. Coat. Technol.*, 2017, **332**, 153–160.
20 Z. Jia, T. Chen, J. Wang, *et al.*, *Tribol. Int.*, 2015, **88**, 17–24.
21 R. Sedlák, A. Kovalčíková, J. Balko, *et al.*, *Int. J. Refract. Met. Hard Mater.*, 2017, **65**, 57–63.
22 C. Shivani, P. M. Harshal, P. K. Om, *et al.*, *J. Mater. Chem.*, 2012, **39**, 21032–21039.
23 S. Xia, Y. Liu, F. Pei, *et al.*, *Polymer*, 2015, **64**, 62–68.
24 W. Zhai, X. Shi, J. Yao, *et al.*, *Composites, Part B*, 2015, **70**, 149–155.
25 H. Liu, Y. Li, T. Wang, *et al.*, *J. Mater. Sci.*, 2012, **47**(4), 1867–1874.
26 V. Georgakilas, M. Otyepka, A. B. Bourlinos, *et al.*, *Chem. Rev.*, 2012, **112**(11), 6156–6214.
27 P. Lian, J. Wang, D. Cai, *et al.*, *Electrochim. Acta*, 2014, **116**, 103–110.
28 J. Hwang, T. Yoon, S. H. Jin, *et al.*, *Adv. Mater.*, 2013, **25**, 6724–6729.
29 H. W. Ha, A. Choudhury, T. Kamal, *et al.*, *ACS Appl. Mater. Interfaces*, 2012, **4**, 4623–4630.
30 W. Zhai, N. Srikanth, L. Kong, *et al.*, *Carbon*, 2017, **119**, 150–171.
31 H. Kinoshita, Y. Nishina, A. A. Alias, *et al.*, *Carbon*, 2014, **66**, 720–723.
32 Y. Peng, Z. Wang and K. Zou, *Langmuir*, 2015, **31**, 7782–7791.
33 H. Wang, T. Maiyalagan, X. Wang, *et al.*, *ACS Catal.*, 2012, **2**, 781–794.
34 L. Niu, Z. Li, W. Hong, *et al.*, *Electrochim. Acta*, 2013, **108**, 666–673.
35 X. Ye, L. Ma, Z. Yang, *et al.*, *ACS Appl. Mater. Interfaces*, 2016, **8**, 7483–7488.
36 P. Wu, X. Li, C. Zhang, *et al.*, *ACS Appl. Mater. Interfaces*, 2017, **9**, 21554–21562.
37 J. Ou, J. Wang, S. Liu, *et al.*, *Langmuir*, 2010, **26**(20), 15830–15836.
38 Z. Wei, D. Wang, S. Kim, *et al.*, *Science*, 2010, **328**(5984), 1373–1376.
39 Y. Li, K. Sheng, W. Yuan, *et al.*, *Chem. Commun.*, 2013, **49**, 291–293.
40 X. Zhang, X. Fan, C. Yan, *et al.*, *ACS Appl. Mater. Interfaces*, 2012, **4**(3), 1543–1552.
41 X. Ji, Y. Xu, W. Zhang, *et al.*, *Composites, Part A*, 2016, **87**, 29–45.
42 Z. Xu and C. Gao, *Nat. Commun.*, 2011, 571, DOI: 10.1038/ncomms1583.
43 C. C. Teng, C. M. Ma, C. H. Lu, *et al.*, *Carbon*, 2011, **49**(15), 5107–5116.
44 J. M. Englert, C. Dotzer, G. Yang, *et al.*, *Nat. Chem.*, 2011, **3**, 279–286.
45 H. J. Salavagione, G. Martinez, G. Ellis, *et al.*, *Macromol. Rapid Commun.*, 2011, **32**(22), 1771–1789.
46 F. M. Koehler, A. Jacobsen, K. Ensslin, *et al.*, *Small*, 2010, **6**(10), 1125–1130.
47 V. Georgakilas, M. Otyepka, A. B. Bourlinos, *et al.*, *Chem. Rev.*, 2012, **112**(11), 6156–6214.
48 K. P. Furlan, J. D. Mello, A. N. Klein, *et al.*, *Tribol. Int.*, 2018, **120**, 280–298.
49 M. Zhang, B. Chen, J. Yang, *et al.*, *RSC Adv.*, 2015, **5**, 89682–89688.
50 Z. Chen, H. Yan, L. Guo, *et al.*, *Composites, Part A*, 2019, **121**, 18–27.
51 G. Nie, L. Zhang, X. Lu, *et al.*, *Dalton Trans.*, 2013, **38**, 14006–14013.
52 X. Liu, L. Pan, T. Lv, *et al.*, *Chem. Commun.*, 2011, **47**, 11984–11986.
53 A. Fakhri and D. S. Kahi, *J. Photochem. Photobiol., B*, 2017, **166**, 259–263.
54 M. Zhang, B. Chen, H. Tang, *et al.*, *RSC Adv.*, 2015, **5**, 1417–1423.
55 J. Xie, S. Liu, G. Cao, *et al.*, *Nano Energy*, 2013, **2**(1), 49–56.
56 P. Kuang, M. He, H. Zou, *et al.*, *Appl. Catal., B*, 2019, **254**, 15–25.
57 S. Zhang, J. Yang, B. Chen, *et al.*, *Surf. Coat. Technol.*, 2017, **326**, 87–95.
58 H. Song, X. Jia, N. Li, *et al.*, *J. Mater. Chem.*, 2012, **22**, 895–902.
59 C. Liu, H. Yan, Q. Lv, *et al.*, *Carbon*, 2016, **102**, 145–153.

60 C. F. G. Gonzalez, A. Smirnov, A. Centeno, *et al.*, *Ceram. Int.*, 2015, **41**, 7434–7438.
61 S. Du, J. Sun and P. Wu, *Carbon*, 2018, **140**, 338–351.
62 P. Hvizdos, J. Dusza and C. Balazsi, *J. Eur. Ceram. Soc.*, 2013, **33**, 2359–2364.
63 D. H. Cho, J. S. Kim, S. H. Kwon, *et al.*, *Wear*, 2013, **302**, 981–986.
64 Y. Liu, *Master thesis*, Deakin University, USA, 2017.
65 Z. Jia, T. Chen, J. Wang, *et al.*, *Tribol. Int.*, 2015, **88**, 17–24.
66 Y. Meng, F. Su and Y. Chen, *ACS Appl. Mater. Interfaces*, 2017, **9**, 39549–39559.
67 X. Liu, X. Shi, Y. Huang, *et al.*, *Mater. Chem. Phys.*, 2018, **213**, 368–373.
68 Y. Meng, F. Su and Y. Chen, *ACS Appl. Mater. Interfaces*, 2015, **7**, 11604–11612.
69 T. K. Meysam, O. Emad, L. M. Pradeep, *et al.*, *Engineering Science and Technology, an International Journal*, 2016, **19**, 463–469.
70 Z. Liu, D. Shu, P. Li, *et al.*, *RSC Adv.*, 2014, **4**, 15937–15944.
71 Z. Xu, X. Shi, W. Zhai, *et al.*, *Carbon*, 2014, **67**, 168–177.
72 H. Song, Z. Wang, J. Yang, *et al.*, *Chem. Eng. J.*, 2017, **324**, 51–62.
73 X. Shen, X. Pei, Y. Liu, *et al.*, *Composites, Part B*, 2014, **57**, 120–125.
74 D. Liu, W. Zhao, S. Liu, *et al.*, *Surf. Coat. Technol.*, 2016, **286**, 354–364.
75 W. Shang, T. Cai, Y. Zhang, *et al.*, *Tribol. Int.*, 2018, **118**, 373–380.
76 M. Yang, Z. Zhang, J. Yuan, *et al.*, *RSC Adv.*, 2016, **6**, 110070–110076.
77 L. Javier, R. M. Benito, M. Pilar, *et al.*, *J. Eur. Ceram. Soc.*, 2016, **36**, 429–435.
78 H. P. Mungse, K. Gupta, R. Singh, *et al.*, *J. Colloid Interface Sci.*, 2019, **541**, 150–162.
79 G. Zhang, Y. Hu, X. Xiang, *et al.*, *Tribol. Int.*, 2018, **126**, 39–48.
80 J. Ou, Y. Wang, J. Wang, *et al.*, *J. Phys. Chem. C*, 2011, **115**, 10080–10086.
81 Y. Mo, A. Chau, Y. Wan, *et al.*, *Carbon*, 2013, **65**, 261–268.
82 A. Wolk, M. Rosenthal, S. Neuhaus, *et al.*, *Sci. Rep.*, 2018, 5843, DOI: 10.1038/s41598-018-24062-2.
83 C. Liu, Y. Dong, Y. Lin, *et al.*, *Composites, Part B*, 2019, **165**, 491–499.
84 Y. Zhang, P. Yu, Y. Qi, *et al.*, *Mater. Lett.*, 2017, **193**, 93–96.
85 G. Paul, S. Shit, H. Hirani, *et al.*, *Tribol. Int.*, 2019, **131**, 605–619.
86 Z. He and P. Alexandridis, *Phys. Chem. Chem. Phys.*, 2015, **17**, 18238–18261.
87 X. Fan, L. Wang and W. Li, *Tribol. Lett.*, 2015, **58**, 1–12.
88 F. Zhao, L. Zhang, G. Li, *et al.*, *Carbon*, 2018, **136**, 309–319.
89 J. Sun, S. Du, Y. Meng, *et al.*, *J. Tribol.*, 2018, **144**(1), 014501.
90 Z. Jia, X. Pang, H. Li, *et al.*, *Tribol. Int.*, 2015, **90**, 240–247.
91 A. Kundu, R. K. Layek and A. K. Nandi, *J. Mater. Chem.*, 2012, **22**, 8139–8144.
92 Y. Mao, Q. Fan, J. Li, *et al.*, *Sens. Actuators, B*, 2014, **203**, 759–765.
93 Z. Tai, Y. Cheng, Y. An, *et al.*, *Tribol. Lett.*, 2012, **46**, 55–63.
94 G. P. Dimitrios, A. K. Ian and J. Y. Robert, *Compos. Sci. Technol.*, 2016, **137**, 44–51.
95 H. Wang, G. Xie, Z. Zhu, *et al.*, *Composites, Part A*, 2014, **67**, 268–273.
96 S. S. Kandanur, M. A. Rafiee, F. Yavari, *et al.*, *Carbon*, 2012, **50**, 3178–3183.
97 X. Li, H. Lu, J. Li, *et al.*, *Tribol. Int.*, 2018, **127**, 351–360.
98 Y. Mo, M. Yang, Z. Lu, *et al.*, *Composites, Part A*, 2013, **54**, 153–158.
99 A. Kumar, B. Behera, G. D. Thakre, *et al.*, *Ind. Eng. Chem. Res.*, 2016, **55**, 8491–8500.
100 Y. Shi, D. Xiong, J. Li, *et al.*, *J. Phys. Chem. C*, 2016, **120**, 19442–19453.
101 Y. Li, Q. Wang, T. Wang, *et al.*, *J. Mater. Sci.*, 2012, **47**, 730–738.
102 Y. Wu, L. Chen, J. Li, *et al.*, *Eur. Polym. J.*, 2017, **89**, 150–161.
103 J. A. Puertolas, M. Castro, J. A. Morris, *et al.*, *Carbon*, 2019, **141**, 107–122.
104 Y. Wang, H. Ji, L. Li, *et al.*, *Tribol. Lett.*, 2015, **60**, 41–47.
105 B. Pan, Y. Xing, J. Liu, *et al.*, *Tribology*, 2011, **30**(2), 151–155.
106 M. Bastiurea, D. Dima, A. Hadar, *et al.*, *Rev. Chim.*, 2018, **6**, 1391–1397.
107 Y. Lei, J. Lu, F. Lu, *et al.*, *Insulation Materials*, 2012, **45**(5), 5–8.
108 B. Pan, S. Peng, S. Song, *et al.*, *Tribol. Lett.*, 2017, **65**, 1–14.
109 C. Min, P. Nie, H. Song, *et al.*, *Tribol. Int.*, 2014, **80**, 131–140.
110 M. Mo, W. Zhao, Z. Chen, *et al.*, *RSC Adv.*, 2015, **5**, 56486–56497.
111 X. Shen, X. Pei, S. Fu, *et al.*, *Polymer*, 2013, **54**, 1234–1242.
112 P. Li, Y. Zheng, T. Shi, *et al.*, *Carbon*, 2016, **96**, 40–48.
113 H. Li, L. Jin, J. Dong, *et al.*, *RSC Adv.*, 2016, **6**, 60200–60205.
114 Q. Lin, L. Qu, Q. Lu, *et al.*, *Polym. Test.*, 2013, **32**, 330–337.
115 N. Snsari, F. Nazari and F. Illas, *Carbon*, 2016, **96**, 911–918.
116 E. Koren and U. Duerig, *Phys. Rev. B*, 2016, **93**, 201404.
117 P. Wang, M. Hirose, Y. Suzuki, *et al.*, *Surf. Coat. Technol.*, 2013, **221**, 163–172.
118 Z. Gong, J. Shi, B. Zhang, *et al.*, *Carbon*, 2017, **116**, 310–317.
119 P. Saravanan, R. Selyanchyn, M. Watanabe, *et al.*, *Tribol. Int.*, 2018, **127**, 255–263.
120 P. Saravanan, R. Selyanchyn, H. Tanaka, *et al.*, *Carbon*, 2017, **122**, 395–403.
121 Y. Wang, K. Gao, B. Zhang, *et al.*, *Carbon*, 2018, **137**, 49–56.
122 H. Buch, A. Rossi, S. Forti, *et al.*, *Nano Res.*, 2018, **11**(11), 5946–5956.
123 J. Li, J. Li and J. Luo, *Adv. Sci.*, 2018, **5**, 1800810–1800817.
124 X. Feng, S. Kwon, J. Y. Park, *et al.*, *ACS Nano*, 2013, **7**(2), 1718–1724.
125 L. Wang, X. Zhou, T. Ma, *et al.*, *Nanoscale*, 2017, **9**, 10846–10853.
126 D. Mandelli, I. Leven, O. Hod, *et al.*, *Sci. Rep.*, 2017, **7**, 10851–10860.
127 J. Li, X. Ge and J. Luo, *Carbon*, 2018, **138**, 154–160.
128 X. Ge, J. Li, R. Luo, *et al.*, *ACS Appl. Mater. Interfaces*, 2018, **10**, 40863–40870.
129 X. He, H. Xiao, H. Choi, *et al.*, *Colloids Surf., A*, 2014, **452**, 32–38.
130 Y. Xu, Y. Peng, K. D. Dearn, *et al.*, *Wear*, 2015, **342–343**(3), 297–309.

131 R. Rosentsveig, A. Gorodnev, N. Feuerstein, *et al.*, *Tribol. Lett.*, 2009, **36**(2), 175–182.
132 M. Ratoi, V. B. Niste, J. Walker, *et al.*, *Tribol. Lett.*, 2013, **52**(1), 81–91.
133 K. Zhang, H. P. Li, Q. Shi, *et al.*, *Chalcogenide Lett.*, 2015, **12**(2), 51–57.
134 H. T. Q. Shi, H. Zhu, G. Tang, *et al.*, *Chalcogenide Lett.*, 2014, **11**(5), 199–207.
135 P. Li, H. Zhou and X. Cheng, *Appl. Surf. Sci.*, 2013, **285**, 937–944.
136 X. Zeng, Y. Peng and H. Lang, *Carbon*, 2017, **118**, 233–240.
137 D. Shu, H. Gao and D. Zhang, *Key Eng. Mater.*, 2016, **693**, 566–575.
138 B. J. Robinson, N. D. Kay and O. V. Kolosov, *Langmuir*, 2013, **29**, 7735–7742.
139 D. Berman, A. Erdemir, A. V. Zinovev, *et al.*, *Diamond Relat. Mater.*, 2019, **54**, 91–96.
140 L. Xu, Y. Zheng, Z. Yan, *et al.*, *Appl. Surf. Sci.*, 2016, **370**, 201–208.
141 M. E. Foo and S. C. B. Gopinath, *Biomed. Pharmacother.*, 2017, **94**, 354–361.
142 Z. Li, N. W. Khun, *et al.*, *J. Mech. Behav. Biomed. Mater.*, 2017, **65**, 77–89.
143 F. Cura, A. Mura and F. Adamo, *AIAS 2018 International Conference on Stress Analysis*, 2018, vol. 12, pp. 44–51.
144 G. Paul, H. Hirani, T. Kuila, *et al.*, *Nanoscale*, 2019, **11**, 3458–3483.
145 J. Mao, J. Zhao, W. Wang, *et al.*, *Tribol. Int.*, 2018, **119**, 614–621.
146 A. Mura, F. Cura and F. Adamo, *Tribol. Int.*, 2018, **117**, 162–167.
147 Z. Cheng, W. Li, P. Wu, *et al.*, *J. Alloys Compd.*, 2017, **722**, 778–784.